Linear theory for beams with intermediate piers

Maurizio GARRIONE - Filippo GAZZOLA

Dipartimento di Matematica, Politecnico di Milano

Piazza Leonardo da Vinci, 32 - 20133 Milano, Italy

e-mail addresses: maurizio.garrione@polimi.it, filippo.gazzola@polimi.it

Abstract

The full linear theory for hinged beams with intermediate piers is developed. The analysis starts with the variational setting and the study of the linear stationary problem. Well-posedness results are provided and the possible loss of regularity, due to the presence of the piers, is analyzed. A complete spectral theorem is then proved, explicitly determining the eigenvalues on varying of the position of the piers and exhibiting the fundamental modes of oscillation. A related second order eigenvalue problem is also studied, showing that it may display nonsmooth eigenfunctions and that the fourth order problem cannot be seen as the square of a second order problem.

Keywords: beams, intermediate piers, spectral analysis, multi-point conditions.

AMS 2010 Subject Classification: 34B10, 34L15, 74K10.

1 Introduction

We consider a multiply hinged beam divided in three adjacent spans (segments): the main (middle) span and two side spans separated by piers. Without loss of generality, we normalize the total length to 2π and represent the beam as in Figure 1. The parameters $0 < a, b < 1$ determine the relative measure

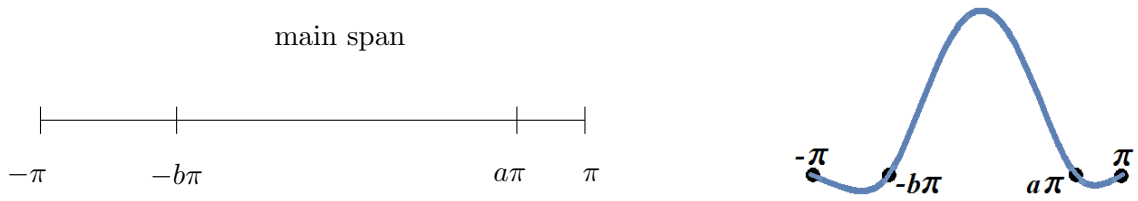

Figure 1: A beam with two piers and $0 < a, b < 1$.

of the side spans with respect to the main span. The beam is hinged at the extremal points $\pm\pi$ and, in correspondence of the positions of the piers, at the points $-b\pi$ and $a\pi$. If $\gamma > 0$ denotes an elastic restoring parameter, the linear evolution equation for this structure reads

$$u_{tt} + u_{xxxx} + \gamma u = 0 \qquad x \in I = (-\pi, \pi), \quad t > 0, \tag{1.1}$$

where u represents the vertical displacement and the equation is meant in a suitable weak sense. Equation (1.1) is complemented with the boundary and internal conditions

$$u(-\pi, t) = u(\pi, t) = u(-b\pi, t) = u(a\pi, t) = 0 \qquad t \geqslant 0. \tag{1.2}$$

The constraints at $\{-b\pi, a\pi\}$ prevent displacements in correspondence of the piers and give rise to a problem for (1.1), for which no standard theoretical framework can be used. The main purpose of this paper is precisely to provide a suitable functional setting for problem (1.1)-(1.2) and therefore we only focus on the linear stationary problem, leaving the nonlinear and evolution problems to a future work [4]; part of this work will be based on [3].

We start with the regularity theory for linear stationary beam equations with a forcing term, namely

$$u'''' + \gamma u = f \quad \text{in } I, \quad u(-\pi) = u(\pi) = u(-b\pi) = u(a\pi) = 0, \tag{1.3}$$

showing that the solutions have to be meant in a suitable weak sense. In fact, one can deal with equation (1.3) in its strong form only if the solution exhibits particular features, see Corollary 4. We stick instead to the weak formulation of (1.3), given by

$$\int_I u''v'' + \gamma \int_I uv = \langle f, v\rangle_V \qquad \forall v \in V(I), \tag{1.4}$$

where the functional space $V(I)$, that takes into account the constraints at the piers, is introduced in Section 2. A strong formulation, not coinciding with (1.3), is given at the end of Section 2.1. Both (1.3) and (1.4) fit in the framework of the so-called *multi-point* problems for ODE's, that were introduced in the pioneering work by Wilder [13], see also [10] for some developments in the subsequent decades. However, as far as we are aware, there are no established results concerning (1.3) or (1.4), neither concerning a precise weak formulation nor providing qualitative properties of the solutions. Also the spectral analysis is completely missing. In fact, the research on multi-point fourth order ODE's has mostly focused on the search for positive solutions for nonlinear equations (through topological methods) and on numerical schemes for approximation of the solutions. The only contributions in literature (weakly) related to the present investigation seem to be [7, 8].

We continue with the spectral analysis of the eigenvalue problem

$$u'''' = \lambda u \quad \text{in } I, \quad u(-\pi) = u(\pi) = u(-b\pi) = u(a\pi) = 0, \tag{1.5}$$

giving a complete picture of the eigenvalues and of the associated eigenfunctions, whose nodal properties are described in detail. Also here it is necessary to consider the equation in weak sense, as in Section 3. This requires a sound variational setting based on classical principles of functional analysis and basic theory of linear differential equations.

Finally, we will show that, due to the presence of the piers, the fourth order eigenvalue problem (1.5) *is not the square of a second order eigenvalue problem*, making the spectral analysis even more delicate.

The underlying motivation for studying equation (1.1) is a quantitative analysis of the instability of suspension bridges with respect to the position of the piers. However, two main ingredients are missing in (1.1): the possibility of displaying torsional oscillations and some nonlinearity which is intrinsic in complicated elastic structures such as bridges (nonlinearity in beams displays several unexpected phenomena, see e.g. [2, 5]). We will reach a reliable bridge model elsewhere [4]; nevertheless, even in the simplified setting of the present paper, we will see that the two internal conditions in the piers create an interaction between the three spans as in real suspension bridges, see [6], to be compared with the right picture in Figure 1. Due to the extreme complexity of the asymmetric case ($b \neq a$), at some point we restrict our attention to the case of symmetric beams ($b = a$), also motivated by the fact that most suspension bridges have equal side spans.

The paper is organized as follows. In Section 2 we deal with the variational formulation of the linear stationary beam equation. This requires the introduction of new functional spaces; in Theorem 1, we show that they are subspaces of codimension two of the Sobolev space $H^2 \cap H_0^1(I)$ and we fully characterize them. The two missing dimensions prevent a nice regularity theory for weak solutions: in Theorem 3 we show why, in general, one cannot expect to have more than C^2-smoothness, the reason

being that the piers yield impulses on the beam, to be added to most forcing terms. In Corollary 4 we provide a simple way to recognize the cases where the weak solution is also a classical solution. In Section 3, our linear analysis tackles the spectral properties of the fourth order differential operator. Also for the eigenvalue problem (1.5) we cannot expect regularity of the eigenfunctions and standard forms of Sturm-Liouville-type results fail. Therefore, we proceed "by hand". A full description of the spectrum is extremely complicated, see Theorem 5; since most suspension bridges have equal side spans, we restrict our attention to the symmetric case $b = a$ with equal side spans, for which simpler properties hold. By taking advantage of symmetries, in Theorem 6 we determine explicitly all the eigenvalues of (1.5) and the associated eigenfunctions. They strongly depend on the position of the piers, as described in Theorems 8 and 10, which also characterize the placement and the number of zeros of the eigenfunctions. The pattern of "zeros moving on the spans" has an elegant form, which is depicted in Figures 9 and 10. In Section 4 we show that, for the second order eigenvalue problem $-u'' = \mu u$, with the same constraints as in (1.5), the eigenfunctions may be nonsmooth and the eigenvalues may be either simple, double or triple. Not only this highlights a profound difference with the fourth order problem, but also that the second order problem is not its "squared root". All the proofs are given in Section 5. At the end of the paper, we draw the conclusions and suggest some future developments.

2 The functional setting for linear beams

We consider a hinged beam of length 2π, represented by the segment $I = (-\pi, \pi)$, which has two intermediate piers in correspondence of the points $-b\pi$ and $a\pi$, $0 < a, b < 1$. We set

$$I_- = (-\pi, -b\pi), \qquad I_0 = (-b\pi, a\pi), \qquad I_+ = (a\pi, \pi),$$

so that $\overline{I} = \overline{I}_- \cup \overline{I}_0 \cup \overline{I}_+$. The aim of this section is to provide a functional framework in which problem (1.1)-(1.2) can be settled.

2.1 Weak solutions and regularity

In order to study both the functional setting and the regularity of the solutions of (1.4), we introduce the space

$$V(I) := \{u \in H^2 \cap H_0^1(I);\, u(-b\pi) = u(a\pi) = 0\}\,, \tag{2.1}$$

endowed with the scalar product $(u, v) \mapsto \int_I u''v''$. Notice that the boundary and internal conditions

$$u(-\pi) = u(\pi) = u(-b\pi) = u(a\pi) = 0 \tag{2.2}$$

make sense since $V(I)$ embeds into $C^0(\overline{I})$. We characterize $V(I)$ by observing that it has codimension two, since the conditions $u(-b\pi) = u(a\pi) = 0$ impose two independent constraints in the Fourier expansion of any element of $V(I)$ in $H^2 \cap H_0^1(I)$. Defining

$$v_1(x) = \begin{cases} -(b+1)\big(x^3 + 3\pi x^2 + \pi^2(b^2+2b)x + \pi^3(b^2+2b-2)\big) & x \in [-\pi, -b\pi] \\ (1-b)\big(x^3 - 3\pi x^2 + \pi^2(b^2-2b)x - \pi^3(b^2-2b-2)\big) & x \in [-b\pi, \pi] \end{cases} \tag{2.3}$$

and

$$v_2(x) = \begin{cases} (a-1)\big(x^3 + 3\pi x^2 + \pi^2(a^2-2a)x + \pi^3(a^2-2a-2)\big) & x \in [-\pi, a\pi] \\ (1+a)\big(x^3 - 3\pi x^2 + \pi^2(a^2+2a)x - \pi^3(a^2+2a-2)\big) & x \in [a\pi, \pi], \end{cases} \tag{2.4}$$

it can be seen that v_1 and v_2 generate $V(I)^\perp$, since for every $u \in V(I)$ one has

$$\int_I u''v_1'' = 12u(-b\pi) = 0, \qquad \int_I u''v_2'' = 12u(a\pi) = 0.$$

This proves the following statement.

Theorem 1. *The space $V(I)$ defined in (2.1) is a subspace of $H^2 \cap H_0^1(I)$ having codimension 2, whose orthogonal complement is given by*

$$V(I)^\perp = \{v \in C^2(\overline{I}) \mid v(\pm\pi) = v''(\pm\pi) = 0,\ v'' \text{ is piecewise affine on } \overline{I}_-, \overline{I}_0 \text{ and } \overline{I}_+\}.$$

Therefore, $V(I)^\perp \cap C^3(I) = \{0\}$.

Notice that $V(I)^\perp$ is made by functions that are more regular than $H^2(I)$; they are $C^2(\overline{I})$, but they fail to be C^3 (except for the zero function) since each pier produces a discontinuity in the third derivative. This effect is well seen by looking into expressions (2.3) and (2.4). Notice that the basis $\{v_1(x), v_2(x)\}$ is not orthogonal, but it has the advantage of highlighting separately the two singularities at the piers. We will complement Theorem 1 by determining an explicit orthogonal basis of $V(I)$ in Theorem 8: all the elements of this basis will be of class $C^2(\overline{I})$, some of them may even be analytic. In Figure 2 we represent the graphs of v_1 and v_2, as well as their second derivatives, in the case $b = 3/4$ and $a = 1/4$. The plots for other values of a and b, possibly different, are qualitatively similar.

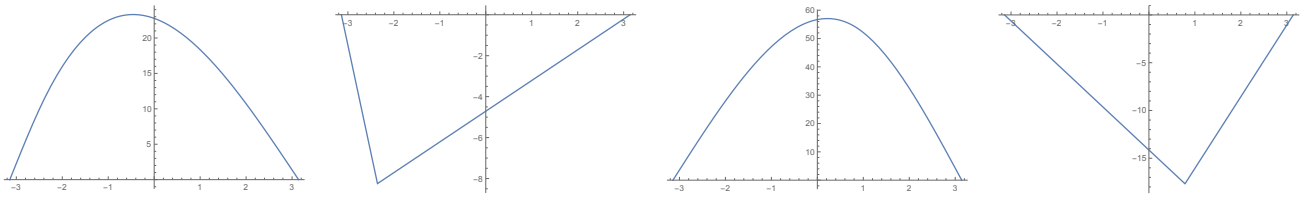

Figure 2: From left to right: plots of the functions v_1, v_1'', v_2, v_2'' in the case $b = 3/4$ and $a = 1/4$.

We incidentally observe that the orthogonal complement of $H_0^2(I)$ in $H^2 \cap H_0^1(I)$ is spanned by the two functions $\pi^2 - x^2$, $x(\pi^2 - x^2)$, whose second derivatives (-2 and $-6x$) are, respectively, the limits in $L^2(I)$ when $a, b \to 1$ of

$$\frac{v_1''(x)}{6\pi(1-b)} + \frac{v_2''(x)}{6\pi(1-a)} \qquad \text{and} \qquad -\frac{v_1''(x)}{2(1-b)} + \frac{v_2''(x)}{2(1-a)}.$$

On the other hand, when $a, b \to 0$ the space $V(I)$ "converges" to the limit space

$$V_*(I) := \{u \in H^2 \cap H_0^1(I);\ u(0) = u'(0) = 0\}, \tag{2.5}$$

whose orthogonal complement $V_*(I)^\perp$ in $H^2 \cap H_0^1(I)$ is spanned by functions w_1 and w_2 having second derivatives

$$w_1''(x) = \begin{cases} x + \pi & \text{if } -\pi \leqslant x \leqslant 0 \\ \pi - x & \text{if } 0 \leqslant x \leqslant \pi, \end{cases} \qquad w_2''(x) = \begin{cases} x + \pi & \text{if } -\pi \leqslant x < 0 \\ x - \pi & \text{if } 0 < x \leqslant \pi. \end{cases}$$

These functions are obtained, respectively, as limits in $L^2(I)$ when $a, b \to 0$ of

$$-\frac{v_1''(x)}{6} \qquad \text{and} \qquad \frac{b-a-2}{12(1-b)(a+b)}\, v_1''(x) + \frac{2+b-a}{12(1-a)(a+b)}\, v_2''(x).$$

In fact, v_1'' and v_2'' have the same L^2-limit. Note also that w_1'' is continuous, while w_2'' is not. Hence, contrary to $V(I)^\perp$, the space $V_*(I)^\perp$ contains functions which *are not* C^2.

We now pass to study the forced stationary version of (1.1). First, we recall that if there are no piers, the equation reads as

$$u''''(x) + \gamma u(x) = f(x) \qquad x \in I \tag{2.6}$$

and the natural functional space where solutions of (2.6) have to be sought is $H^2 \cap H_0^1(I)$ endowed with the same scalar product. The notion of weak solution is then derived from a variational principle: the total energy $E(u)$ of the beam in position u is the sum of the bending energy, the restoring energy, and the forcing energy.

If the beam does have intermediate piers, the energy is defined on the functional space $V(I)$, that is,

$$E(u) = \frac{1}{2}\int_I \Big((u'')^2 + \gamma u^2\Big) - \langle f, u\rangle_V \qquad \forall u \in V(I), \tag{2.7}$$

where $\langle\cdot,\cdot\rangle_V$ denotes the duality pairing between $V(I)$ and $V'(I)$, its dual space. If $f \in L^1(I)$, then the duality may be replaced by the integral $\int_I fu$. By computing the Fréchet derivative of E in $V(I)$, we obtain the following definition.

Definition 2. *Let $f \in V'(I)$. We say that $u \in V(I)$ is a weak solution of (2.6)-(2.2) if*

$$\int_I u''v'' + \gamma\int_I uv = \langle f, v\rangle_V \qquad \forall v \in V(I). \tag{2.8}$$

In the sequel, we denote by $\delta_{-b\pi}, \delta_{a\pi} \in V'(I)$ the Dirac delta distributions at the points $-b\pi$ and $a\pi$. In the next statement, which will be proved in Section 5.1, we discuss the regularity of weak solutions.

Theorem 3. *Let $\gamma \geqslant 0$. For all $f \in V'(I)$ there exists a unique weak solution $u \in V(I)$ of (2.6)-(2.2), according to Definition 2. Moreover, if $f \in C^0(\overline{I})$, then:*

(i) the solution satisfies $u \in C^4(\overline{I}_-) \cap C^4(\overline{I}_0) \cap C^4(\overline{I}_+) \cap C^2(\overline{I})$ and $u''(\pm\pi) = 0$;

(ii) there exist $\alpha_f, \beta_f \in \mathbb{R}$ (depending on f, γ, a, b) such that $u'''' + \gamma u = f + \alpha_f\delta_{a\pi} + \beta_f\delta_{-b\pi}$ in distributional sense;

(iii) there exists a subspace $X(I) \subset C^0(\overline{I})$ of codimension 2 such that $u \in C^4(\overline{I})$ if and only if $f \in X(I)$;

(iv) we have that $u \in C^4(\overline{I})$ if and only if $u \in C^3(\overline{I})$.

From Item *(i)* we see that a weak solution of (2.8) makes the beam globally hinged: its least energy configuration is C^2 at the piers and displays no bending at the endpoints. This may lead to nonsmooth solutions of (2.8): indeed, Item *(ii)* says that

if the two-piers beam is subject to a continuous force f,
then each pier yields an additional load equal to some impulse depending on f.

The procedure that we develop in the proof of Item *(ii)* explains why, in most cases, the regularity of the solution cannot be improved to $C^4(\overline{I})$. In particular, it entails the following statement.

Corollary 4. *Let $\gamma \geqslant 0$ and $f \in C^0(\overline{I})$. Then the weak solution of (2.6)-(2.2) belongs to $C^4(\overline{I})$ if and only if it coincides with the unique classical solution U_f of the problem*

$$U_f''''(x) + \gamma U_f(x) = f(x) \qquad x \in I, \qquad U_f(-\pi) = U_f(-b\pi) = U_f(a\pi) = U_f(\pi) = 0. \tag{2.9}$$

We finally observe that (2.6)-(2.2) may also be written in a "piecewise strong form", by setting

$$u(x) = \begin{cases} u_-(x) & x \in I_- \\ u_0(x) & x \in I_0 \\ u_+(x) & x \in I_+ \end{cases}$$

and splitting the equation and the boundary conditions as follows:

$$\begin{cases} u_-(-\pi) = u_-''(-\pi) = 0 \\ u_-''''(x) + \gamma u_-(x) = f(x) \qquad x \in I_- \\ u_-(-b\pi) = u_0(-b\pi) = 0,\ u_-'(-b\pi) = u_0'(-b\pi),\ u_-''(-b\pi) = u_0''(-b\pi) \\ u_0''''(x) + \gamma u_0(x) = f(x) \qquad x \in I_0 \\ u_0(a\pi) = u_+(a\pi) = 0,\ u_0'(a\pi) = u_+'(a\pi),\ u_0''(a\pi) = u_+''(a\pi) \\ u_+''''(x) + \gamma u_+(x) = f(x) \qquad x \in I_+ \\ u_+(\pi) = u_+''(\pi) = 0. \end{cases}$$

If $f \in C^0(\overline{I})$, such a formulation coincides with the one given in Item (ii) of Theorem 3.

2.2 Examples and further remarks

We illustrate here the procedure mentioned in the previous subsection, applied to two simple and instructive examples helping to better understand the statement of Theorem 3.

- Take $\gamma = 0$ and consider (2.6) with constant load, that is,

$$u''''(x) = 24 \qquad x \in I_- \cup I_0 \cup I_+, \tag{2.10}$$

whose solutions are fourth order polynomials. If (2.10) is complemented with the boundary and internal conditions (2.2), then the function U_f defined by (2.9) is given by

$$U_f(x) = (x + b\pi)(x - a\pi)(x^2 - \pi^2)$$

which *does not satisfy* (2.8), regardless of the values of $a, b < 1$. To see this, it suffices to notice that

$$U_f''(-\pi) = 2\pi^2(5 - 3b + 3a - ab) > 0, \quad U_f''(\pi) = 2\pi^2(5 + 3b - 3a - ab) > 0 \qquad \forall a, b < 1,$$

violating the no-bending boundary behavior in Item (i) of Theorem 3. In Figure 3 we plot the graphs of the functions U_f and of the weak solution $\overline{u}$ of (2.10) when $b = 0.5$ and $a = 0.7$: their difference is quite evident.

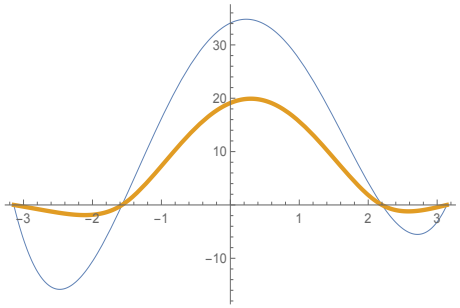

Figure 3: Plots of U_f (thin line) and of the weak solution $\overline{u}$ of (2.10) (thick line) for $b = 0.5$, $a = 0.7$.

The function $\overline{u}$, as characterized by Definition 2, may be obtained through the procedure explained in the proof of Theorem 3. This solution minimizes the energy defined in (2.7): let us define

$$H(a, b) := E(U_f) - E(\overline{u}) \qquad \forall (a, b) \in (0, 1)^2. \tag{2.11}$$

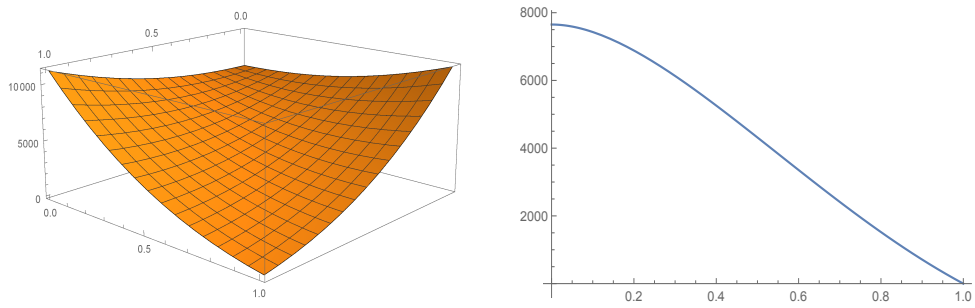

Figure 4: Plots of $(a,b) \mapsto H(a,b)$ on $(0,1)^2$ (left) and of $a \mapsto H(a,a)$ on $(0,1)$ (right).

Then $H(a,b) > 0$ in the square $(0,1)^2$ and the graph of the map $(a,b) \mapsto H(a,b)$ is plotted in the left picture in Figure 4. It turns out that $0 = H(1,1) < H(a,b) < H(1,0) = H(0,1)$ for all $(a,b) \in (0,1)^2$. Moreover, the graph is obviously symmetric with respect to the line $a = b$: in the right picture of Figure 4 we plot the graph of the map $a \mapsto H(a,a) = \frac{(5-a^2)^2(1+2a-3a^2)\pi^5}{2a+1}$ for $a \in (0,1)$, which corresponds to beams with symmetric side spans. Since $\overline{u} \neq U_f$ for all a, b, it never occurs that $(\alpha_f, \beta_f) = (0,0)$ and therefore the constant load $f(x) = 24$ does not belong to the subspace $X(I)$ introduced in Item (iii) of Theorem 3. Clearly, the coefficients α_f and β_f depend on a and b; in Figure 5 we plot the graphs of

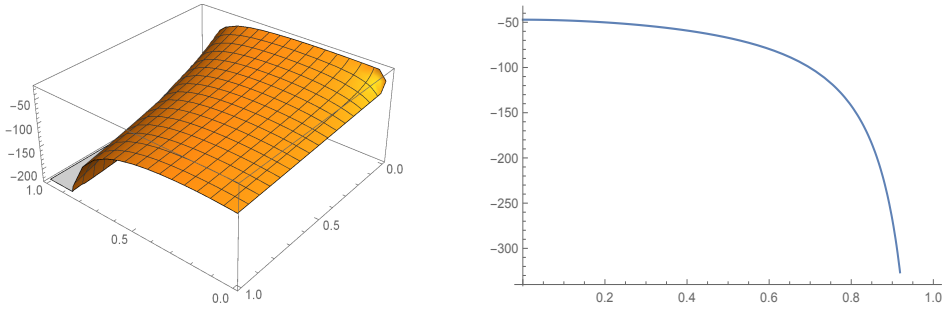

Figure 5: Plots of $(a,b) \mapsto \beta_f(a,b)$ on $(0,1)^2$ (left) and of $a \mapsto \beta_f(a,a)$ on $(0,1)$ (right).

the map $(a,b) \mapsto \beta_f(a,b)$ for $(a,b) \in (0,1)^2$ and of the map $a \mapsto \beta_f(a,a) = \frac{3(1+a)(a^2-5)\pi}{(1-a)(2a+1)}$ for $a \in (0,1)$. Both these functions diverge to $-\infty$ as $a \to 1$, meaning that

the contribution of the piers, in terms of impulses depending on the force f, increases and tends to infinity as the piers approach the endpoints of the beam.

- Take again $\gamma = 0$ and consider now (2.6) with a trigonometric load, that is,

$$u''''(x) = m^4 \sin(mx) \qquad x \in I_- \cup I_0 \cup I_+ \qquad \text{for some integer } m = 2, 3, 4... \,. \tag{2.12}$$

Then,

$$U_f(x) = \sin(mx) + \left[\frac{\sin(bm\pi)}{1-b^2} + \frac{\sin(am\pi)}{1-a^2}\right] \frac{x(x^2-\pi^2)}{(a+b)\pi^3} + \left[\frac{b\sin(am\pi)}{1-a^2} - \frac{a\sin(bm\pi)}{1-b^2}\right] \frac{x^2-\pi^2}{(a+b)\pi^2}.$$

According to Definition 2 and Corollary 4, this function is a weak solution of (2.12) if and only if $U_f''(-\pi) = U_f''(\pi) = 0$. After some computations, one sees that this occurs if and only if $\sin(bm\pi) = \sin(am\pi) = 0$, that is, $b = h/m$ and $a = k/m$ for any couple of integers $h, k \in \{1, ..., m-1\}$. In this case, the weak solution of (2.12) is $\overline{u}(x) = U_f(x) = \sin(mx)$, which is of class $C^4(\overline{I})$; in fact, it is analytic in I. This example tells us that, for some continuous forces f,

the regularity of the solution depends on the relative lengths of the three spans.

Consider again the weak solution $\overline{u}$ of (2.12), as characterized by Definition 2, and the map (2.11). For $m = 3$, in the left picture of Figure 6 we plot the graph of the map $(a, b) \mapsto H(a, b)$ in the square $(0, 1)^2$, while in the right picture therein we plot the graph of the map $a \mapsto H(a, a) = \frac{3(3+a)\sin^2(3a\pi)}{(1-a)a^2(1+a)^2\pi^3}$ for $a \in (0, 1)$. The zeros of these functions are quite visible.

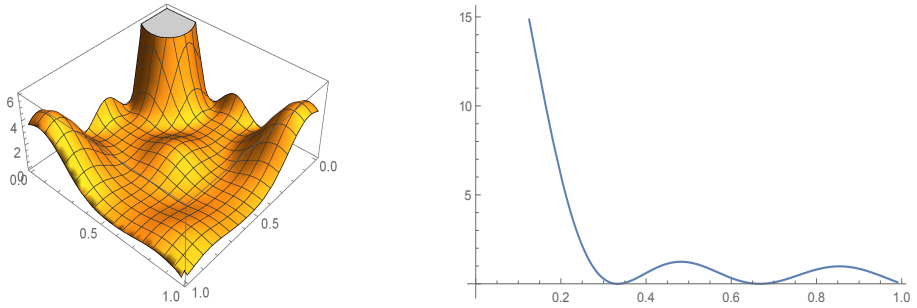

Figure 6: Plots of $(a, b) \mapsto H(a, b)$ on $(0, 1)^2$ (left) and of $a \mapsto H(a, a)$ on $(0, 1)$ (right).

As noticed above, $\overline{u} = U_f$ if and only if $a, b \in \{\frac{1}{3}, \frac{2}{3}\}$: for these four couples, we have $(\alpha_f, \beta_f) = (0, 0)$ and the load $f(x) = 81\sin(3x)$ belongs to the subspace $X(I)$, see Item (iii) of Theorem 3. By emphasizing the dependence $\alpha_f = \alpha_f(a, b)$ and $\beta_f = \beta_f(a, b)$ as above, in Figure 7 we plot the graphs of the map $(a, b) \mapsto \beta_f(a, b)$ for $(a, b) \in (0, 1)^2$ and of the map $a \mapsto \beta_f(a, a) = \frac{3\sin(3a\pi)}{(1-a)^2a^2\pi^3}$ for $a \in (0, 1)$. We observe that $\beta_f(a, a)$ changes its sign in correspondence of $a = 1/3, a = 2/3$: in these cases, $f(\pm a\pi) = 0$. If instead $f > 0$ (resp., $f < 0$) in one pier, then the impulse due to that pier points downwards (resp., upwards), showing that

the piers "resist" to the action of the load f.

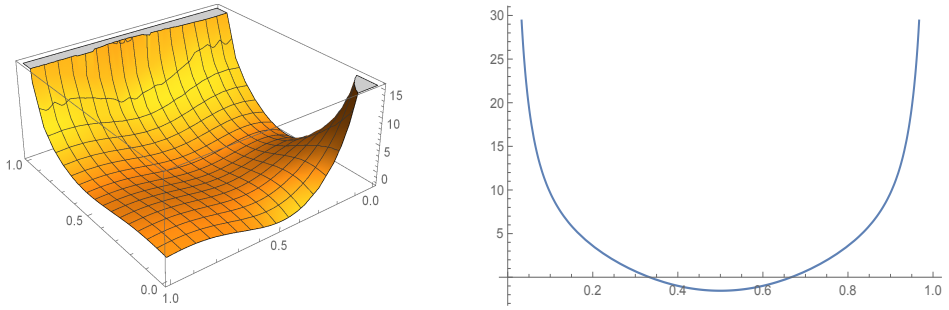

Figure 7: Plots of $(a, b) \mapsto \beta_f(a, b)$ on $(0, 1)^2$ (left) and of $a \mapsto \beta_f(a, a)$ on $(0, 1)$ (right).

As we have just seen, for some continuous forces f the solution is not globally C^4 regardless of a and b, for some other f the solution may be globally C^4 only for particular values of a and b. Moreover, it may happen that $\beta_f = 0$ and $\alpha_f \neq 0$ (or vice versa), in which case $u \in C^4(\overline{I_- \cup I_0}) \cap C^4(\overline{I}_+)$ (resp. $u \in C^4(\overline{I}_-) \cap C^4(\overline{I_0 \cup I_+})$).

• We conclude this section with a simple remark and a related curious example. It is clear that the piers constraint prevents the positivity preserving property to be true. This means that if $\gamma = 0$ and $f \geqslant 0$, one cannot expect the weak solution of (2.8) to satisfy $\overline{u} \geqslant 0$ as in beams with no piers. It is

however of physical interest to investigate which conditions on f yield a nonnegative solution $\overline{u}$. As an example, take $a = b = 1/2$ and consider the functions

$$f(x) = \tfrac{177}{16}\cos(\tfrac{x}{2})\cos^2(x) - 17\cos(x)\sin(x)\sin(\tfrac{x}{2}) - 11\cos(\tfrac{x}{2})\sin^2(x) \quad \text{and} \quad \overline{u}(x) = \cos^2(x)\cos(\tfrac{x}{2}),$$

whose plots are reported in Figure 8.

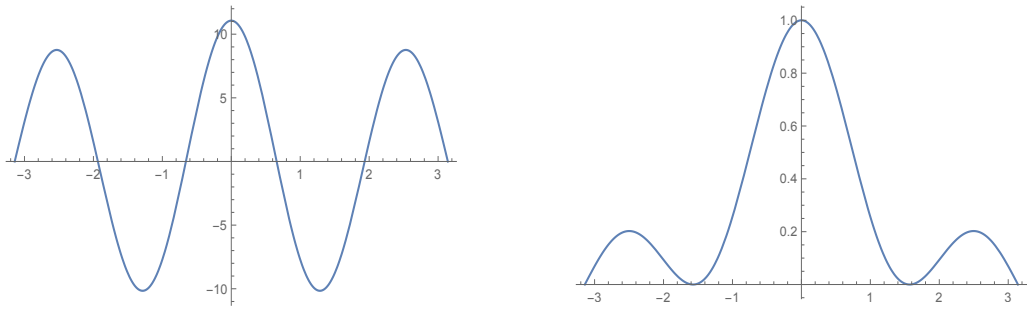

Figure 8: Plots of the functions f (left) and $\overline{u}$ (right).

One can check that $\overline{u}''''(x) = f(x)$ for all $x \in (-\pi, \pi)$ and that $\overline{u}(\pm\pi) = \overline{u}''(\pm\pi) = \overline{u}(\pm\frac{\pi}{2}) = 0$: hence, by Corollary 4, $\overline{u}$ is a classical and positive solution of (2.8). Clearly, one can change the signs of both f and $\overline{u}$ and stick to the convention that

$$u > 0 \text{ corresponds to a } \textbf{downwards} \text{ displacement.} \tag{2.13}$$

The left picture in Figure 8 tells us that

the upwards displacement $\overline{u}$ of the beam with piers is obtained with a sign-changing load f pushing downwards close to the piers and upwards far away from the piers.

3 Spectral theory for beams with two piers

3.1 Vibrating modes

In this section, we determine the modes of vibration for the beam $I = (-\pi, \pi)$ with two intermediate piers placed at $-b\pi$ and $a\pi$. We find the set of the eigenvalues μ and the corresponding eigenfunctions $e \in V(I)$ solving the problem

$$\int_I e''v'' = \mu \int_I ev \qquad \forall v \in V(I). \tag{3.1}$$

Through a regularity argument similar to that in the proof of Theorem 3-(i), one can show that any eigenfunction belongs to $C^2(\overline{I})$ and is of class C^∞ on each span I_-, I_0, I_+. Moreover, it necessarily satisfies the no-bending boundary conditions

$$e''(-\pi) = e''(\pi) = 0$$

at the endpoints of the beam. If $e \in V(I)$ is an eigenfunction, by taking $v = e$ in (3.1) one obtains that *all the eigenvalues are strictly positive.* We thus set $\mu = \lambda^4$ and seek $e \in V(I)$ such that

$$\int_I e''v'' = \lambda^4 \int_I ev \qquad \forall v \in V(I). \tag{3.2}$$

The following result holds; we will provide its proof in Section 5.2.

Theorem 5. *The eigenvalues μ of problem* (3.1) *are given by $\mu = \lambda^4$, for any $\lambda > 0$ solving the following equation:*

$$\begin{aligned}
&\sin(2\lambda\pi)\sinh\left[\lambda(1-b)\pi\right]\sinh\left[\lambda(1-a)\pi\right]\sinh^2\left[\lambda(a+b)\pi\right]\\
&-\sin\left[\lambda(1-a)\pi\right]\sin\left[\lambda(1+a)\pi\right]\sinh\left[\lambda(1-b)\pi\right]\sinh\left[\lambda(1+b)\pi\right]\sinh\left[\lambda(a+b)\pi\right]\\
&+\sin\left[\lambda(1-b)\pi\right]\sin\left[\lambda(1-a)\pi\right]\sin\left[\lambda(a+b)\pi\right]\sinh\left[\lambda(1+b)\pi\right]\sinh\left[\lambda(1+a)\pi\right]\\
&-\sin\left[\lambda(1-b)\pi\right]\sin\left[\lambda(1+b)\pi\right]\sinh\left[\lambda(1-a)\pi\right]\sinh\left[\lambda(1+a)\pi\right]\sinh\left[\lambda(a+b)\pi\right]\\
&+2\sin\left[\lambda(1-b)\pi\right]\sin\left[\lambda(1-a)\pi\right]\sinh\left[\lambda(1-b)\pi\right]\sinh\left[\lambda(1-a)\pi\right]\sinh\left[\lambda(a+b)\pi\right]\\
&-\sin\left[\lambda(1-b)\pi\right]\sin\left[\lambda(1-a)\pi\right]\sin\left[\lambda(a+b)\pi\right]\sinh\left[\lambda(1-b)\pi\right]\sinh\left[\lambda(1-a)\pi\right]=0.
\end{aligned}$$

We omit writing the explicit form of the corresponding eigenfunctions. We give a complete result only in the case of symmetric beams. So, assume that $0 < b = a < 1$ and let

$$I_- = (-\pi, -a\pi), \qquad I_0 = (-a\pi, a\pi), \qquad I_+ = (a\pi, \pi).$$

The symmetry of the position of the piers enables us to seek separately even and odd solutions of (3.2). We obtain the following statement, whose proof will be given in Section 5.3.

Theorem 6. *Let $b = a$. The set of all the eigenvalues $\mu = \lambda^4$ of* (3.1) *is completely determined by the values of $\lambda > 0$ such that*

$$\sin(\lambda\pi)\sinh(\lambda a\pi)\sinh[\lambda(1-a)\pi] = \sinh(\lambda\pi)\sin(\lambda a\pi)\sin[\lambda(1-a)\pi] \tag{3.3}$$

$$\cos(\lambda\pi)\cosh(\lambda a\pi)\sinh[\lambda(1-a)\pi] = \cosh(\lambda\pi)\cos(\lambda a\pi)\sin[\lambda(1-a)\pi]. \tag{3.4}$$

In case (3.3)*, the corresponding eigenfunctions are* ***odd*** *and given by:*

- $\mathbf{O}_\lambda(x) = \sin(\lambda x)$ *if* $\lambda \in \mathbb{N}$ *(implying both* $\lambda a \in \mathbb{N}$ *and* $\lambda(1-a) \in \mathbb{N}$*);*
- *the odd extension of*

$$\mathscr{O}_\lambda(x) = \begin{cases} \dfrac{\sinh[\lambda(1-a)\pi]}{\sinh(\lambda a\pi)}\left(\sinh(\lambda a\pi)\sin(\lambda x) - \sin(\lambda a\pi)\sinh(\lambda x)\right) & \text{if } x \in [0, a\pi] \\ \dfrac{\sin(\lambda a\pi)}{\sin[\lambda(1-a)\pi]}\left(\sin[\lambda(1-a)\pi]\sinh[\lambda(x-\pi)] - \sinh[\lambda(1-a)\pi]\sin[\lambda(x-\pi)]\right) & \text{if } x \in [a\pi, \pi] \end{cases}$$

if $\lambda \notin \mathbb{N}$ *(implying both* $\lambda a \notin \mathbb{N}$ *and* $\lambda(1-a) \notin \mathbb{N}$*).*

In case (3.4)*, the corresponding eigenfunctions are* ***even*** *and given by*

- $\mathbf{E}_\lambda(x) = \cos(\lambda x)$ *if* $\lambda - 1/2 \in \mathbb{N}$ *(implying both* $\lambda a - 1/2 \in \mathbb{N}$ *and* $\lambda(1-a) \in \mathbb{N}$*);*
- *the even extension of*

$$\mathscr{E}_\lambda(x) = \begin{cases} \dfrac{\sinh[\lambda(1-a)\pi]}{\cosh(\lambda a\pi)}\left(\cosh(\lambda a\pi)\cos(\lambda x) - \cos(\lambda a\pi)\cosh(\lambda x)\right) & \text{if } x \in [0, a\pi] \\ \dfrac{\cos(\lambda a\pi)}{\sin[\lambda(1-a)\pi]}\left(\sinh[\lambda(1-a)\pi]\sin[\lambda(\pi-x)] - \sin[\lambda(1-a)\pi]\sinh[\lambda(\pi-x)]\right) & \text{if } x \in [a\pi, \pi] \end{cases}$$

if $\lambda - 1/2 \notin \mathbb{N}$ *(implying both* $\lambda a - 1/2 \notin \mathbb{N}$ *and* $\lambda(1-a) \notin \mathbb{N}$*).*

Some comments about Theorem 6 are in order. Let us notice that the eigenvalues λ^4 associated with the eigenfunctions $\mathbf{O}_\lambda$ and $\mathbf{E}_\lambda$ correspond to the values of λ for which both sides of the equalities (3.3) and (3.4), respectively, vanish. For this reason, in the case of nonsmooth odd and even eigenfunctions it has necessarily to be $\lambda(1-a) \notin \mathbb{N}$, so that $\mathscr{O}_\lambda$ and $\mathscr{E}_\lambda$ are well-defined. Notice that we fix the eigenfunctions to be all positive in $x = 0$ if even, and increasing in $x = 0$ if odd. Here the convention (2.13) plays no role.

We also observe that the eigenfunctions $\mathbf{O}_\lambda$ and $\mathbf{E}_\lambda$ are of class C^∞, while $\mathscr{O}_\lambda$ and $\mathscr{E}_\lambda$ are only C^2. In view of the conditions on λ, no C^∞-eigenfunctions exist if $a \notin \mathbb{Q}$ since, in this case, it cannot be $\lambda \in \mathbb{N}$ and $\lambda a \in \mathbb{N}$ (or $\lambda - 1/2 \in \mathbb{N}$ and $\lambda a - 1/2 \in \mathbb{N}$) at the same time. On the other hand, if $a = p/q$ with $p, q \in \mathbb{N}$ and $g.c.d.(p, q) = 1$, odd C^∞-eigenfunctions appear for $\lambda_r = rq$, for every $r \in \mathbb{N}$. As for even C^∞-eigenfunctions, they exist whenever $a = p/q$, with $g.c.d.(p, q) = 1$ and both p and q are odd; in this case, the eigenvalues are given by $\lambda_r = r + 1/2$, with $r \in \mathbb{N}$ such that $2r + 1$ is a multiple of q. Thus, there are infinitely many regular eigenfunctions if $a \in \mathbb{Q}$, but it may happen that they are all odd (as in the case $a = 1/2$). The C^∞-eigenfunctions $\mathbf{O}_\lambda$ and $\mathbf{E}_\lambda$ satisfy the strong form of the eigenvalue problem

$$e'''' = \lambda^4 e.$$

As for merely C^2-eigenfunctions, by computing explicitly the third derivative we can formally write equation (3.2), as in Item (ii) of Theorem 3. Precisely, we have

$$e'''' = \lambda^4 e + \alpha_\lambda \delta_{a\pi} + \beta_\lambda \delta_{-a\pi},$$

for suitable constants α_λ and β_λ.

Finally, we notice that conditions (3.3) and (3.4) characterize the *couples* (a, λ) such that $\mu = \lambda^4$ is an eigenvalue of (3.1). Since the least eigenvalue $\mu_0 = \lambda_0^4$ of (3.1) satisfies the lower bound

$$\lambda_0^4 = \min_{v \in V(I)} \frac{\int_I (v'')^2}{\int_I v^2} \geqslant \min_{v \in H^2 \cap H_0^1(I)} \frac{\int_I (v'')^2}{\int_I v^2} = \frac{1}{16}, \tag{3.5}$$

the curves implicitly defined by (3.3) and (3.4) in the (a, λ)-plane all lie above the line $\lambda = 1/2$. In the next section, we characterize in full detail all such curves, which are depicted in Figure 9. Notice that the ones representing the odd eigenvalues (in darker color in Figure 9) are symmetric with respect to $a = 1/2$, since (3.3) does not vary when replacing a by $1 - a$.

In the case $a = 1/2$, Theorem 6 takes the following simple form.

Corollary 7. *Let $b = a = 1/2$. The eigenvalues $\mu = \lambda^4$ of (3.1) are completely determined by the values of $\lambda > 0$ such that*

$$\sin(\lambda\pi/2) = 0 \quad \text{or} \quad \tan(\lambda\pi/2) = \tanh(\lambda\pi/2) \quad \text{or} \quad \tan(\lambda\pi) = \tanh(\lambda\pi).$$

In the first case, a corresponding eigenfunction is given by $\mathbf{O}_\lambda(x) = \sin(\lambda x)$, while in the other two cases it is given, respectively, by the odd extension of

$$\mathscr{O}_\lambda(x) = \begin{cases} \dfrac{\sin(\lambda x)}{\sin(\lambda\pi/2)} - \dfrac{\sinh(\lambda x)}{\sinh(\lambda\pi/2)} & \text{if } x \in [0, \pi/2] \\ \dfrac{\sinh[\lambda(x-\pi)]}{\sinh(\lambda\pi/2)} - \dfrac{\sin[\lambda(x-\pi)]}{\sin(\lambda\pi/2)} & \text{if } x \in [\pi/2, \pi], \end{cases}$$

and by the even extension of

$$\mathscr{E}_\lambda(x) = \begin{cases} \tanh\left(\dfrac{\lambda\pi}{2}\right)\left(\cosh\left(\dfrac{\lambda\pi}{2}\right)\cos(\lambda x) - \cos\left(\dfrac{\lambda\pi}{2}\right)\cosh(\lambda x)\right) & \text{if } x \in [0, \pi/2] \\ \operatorname{cotan}\left(\dfrac{\lambda\pi}{2}\right)\left(\sinh\left(\dfrac{\lambda\pi}{2}\right)\sin[\lambda(\pi - x)] - \sin\left(\dfrac{\lambda\pi}{2}\right)\sinh[\lambda(\pi - x)]\right) & \text{if } x \in [\pi/2, \pi]. \end{cases}$$

.

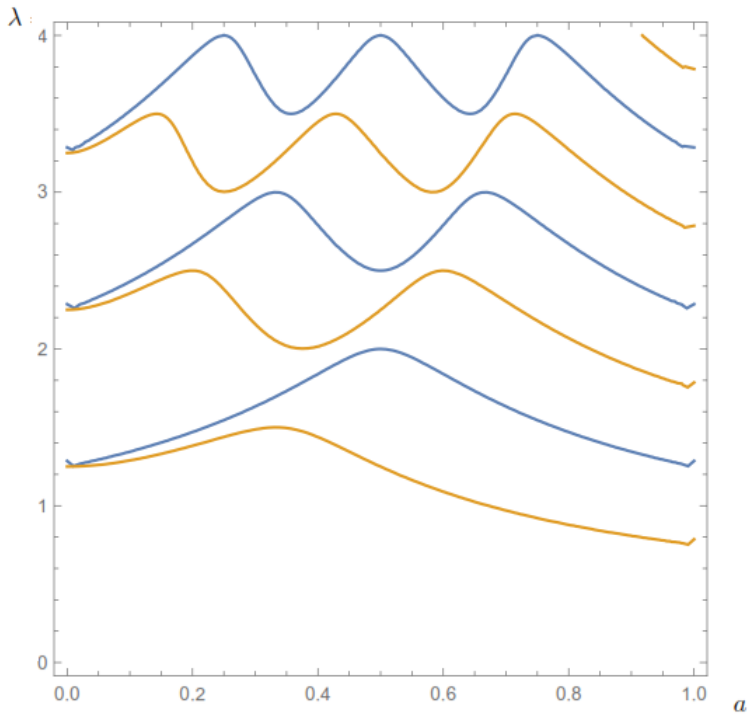

Figure 9: The curves implicitly defined by (3.3)-(3.4) in the region $(a, \lambda) \in (0, 1) \times (0, 4)$.

Therefore, for $b = a = 1/2$, the eigenvalues are given by

$$\lambda = 2k \text{ or } \lambda \approx 2k + \frac{1}{2} \quad \text{(odd)}, \qquad \lambda \approx k + \frac{1}{4} \quad \text{(even)}, \qquad k = 1, 2, \ldots,$$

since the function $s \mapsto \tanh(s)$ rapidly converges to 1.

3.2 Nodal properties of the vibrating modes

The main purpose of this section is to classify the eigenfunctions of problem (3.1), as given in Theorem 6, according to their number of zeros (nodal intervals) in I.

Preliminarily, it is convenient to consider the eigenvalues of the clamped beam on I, that is, the numbers $\mu > 0$ for which the problem

$$\int_I e'' v'' = \mu \int_I ev \qquad \forall v \in H_0^2(I) \tag{3.6}$$

admits a nontrivial solution e. From Section 2.1 we recall that $H_0^2(I)$ is the limit space of $V(I)$ as $a \to 1$. It is straightforward to verify that μ is an eigenvalue of (3.6) if and only if $\mu = \Lambda_n^4$ $(n = 0, 1, 2, \ldots)$, with Λ_n defined by

$$\begin{cases} \tan(\Lambda_{2k}\pi) = -\tanh(\Lambda_{2k}\pi) & \text{with even eigenfunction,} \\ \tan(\Lambda_{2k+1}\pi) = \tanh(\Lambda_{2k+1}\pi) & \text{with odd eigenfunction.} \end{cases} \tag{3.7}$$

The corresponding eigenfunctions ψ_n $(n = 0, 1, 2, \ldots)$ are all of class $C^\infty(I)$ and are explicitly given by

$$\begin{cases} \psi_{2k}(x) = \cosh(\Lambda_{2k}\pi)\cos(\Lambda_{2k}x) - \cos(\Lambda_{2k}\pi)\cosh(\Lambda_{2k}x) \\ \psi_{2k+1}(x) = \sinh(\Lambda_{2k+1}\pi)\sin(\Lambda_{2k+1}x) - \sin(\Lambda_{2k+1}\pi)\sinh(\Lambda_{2k+1}x) \end{cases} \qquad x \in I. \tag{3.8}$$

Moreover, it will be useful to consider also the limit space $V_*(I)$ (as $a \to 0$) introduced in (2.5) and we denote by $\mu = (\Lambda_n^*)^4$ $(n = 0, 1, 2, \ldots)$ the eigenvalues of

$$\int_I e'' v'' = \mu \int_I ev \qquad \forall v \in V_*(I). \tag{3.9}$$

Some computations show that each eigenvalue of (3.9) is double and that

$$\Lambda_n^* = \Lambda_n \quad \text{if } n \text{ is odd}, \qquad \Lambda_n^* = \Lambda_{n+1} \quad \text{if } n \text{ is even}, \tag{3.10}$$

namely the eigenvalues of (3.9) are exactly the eigenvalues of (3.6) with odd index n, all of them having multiplicity 2. The corresponding eigenfunctions are obtained by extending by (even and odd) symmetry the restriction to the interval $[0, \pi]$ of $\psi_{2k+1}(\pi - x)$, where ψ_{2k+1} has been defined in (3.8). Notice, in particular, that the so obtained eigenfunctions of (3.9) are not all of class C^2; in fact, in this case the integration by parts does not imply the matching of the second derivatives in 0, because the test functions v satisfy $v'(0) = 0$, thus canceling the boundary term $u''(0)v'(0)$.

With these preliminaries, we may state the first main result of this section, which will be proved in Section 5.4.

Theorem 8. *For any $a \in (0, 1)$, the eigenvalues $\mu = \lambda^4$ of problem (3.2) are simple and form a countable set, the corresponding eigenfunctions are of class C^2 and form an orthogonal basis of $V(I)$. Moreover, (3.3) and (3.4) implicitly define, for $a \in (0, 1)$, a family of analytic functions $a \mapsto \lambda_n(a)$ which satisfy $\lambda_n(a) \to \Lambda_n$ for $a \to 1$ and $\lambda_n(a) \to \Lambda_n^*$ for $a \to 0$ $(n = 0, 1, 2, \ldots)$.*

We observe that, as a straightforward consequence of Theorem 8, we have

$$\lim_{a \to 0} \frac{\lambda_{n+1}(a)}{\lambda_n(a)} = \begin{cases} 1 & \text{if } n \text{ is even} \\ \dfrac{\Lambda_{n+2}}{\Lambda_n} & \text{if } n \text{ is odd.} \end{cases}$$

Theorem 8 states that the set of couples (a, λ) satisfying either (3.3) or (3.4) is composed by the union of connected branches which are graphs of regular functions $\lambda = \lambda(a)$; their intersections with any line $a = \bar{a} < 1$ give all the eigenvalues $\mu = \lambda^4$ of problem (3.2) corresponding to the choice $a = \bar{a}$, see again Figure 9. It turns out that, even if all the eigenvalues are simple, the spectral gaps can be very small. This means that the associated vibrating modes of the linear evolution equation (1.1) have fairly similar time frequencies.

We now turn to the nodal properties of the eigenfunctions. For a given $a \in (0, 1)$, Theorem 8 allows us to sort the eigenvalues in increasing order $\{\lambda_0, \lambda_1, \lambda_2, \ldots\}$ and to label the associated eigenfunctions as $\{e_0, e_1, e_2, \ldots\}$. We will always speak about *even* and *odd* eigenfunctions and eigenvalues, referring to such labels. The placement of the zeros of the eigenfunctions e_n, depending on the couple (a, λ), is of crucial importance. This was already noticed in the Federal Report on the Tacoma Narrows Bridge collapse, see Drawing 4 in the final pages of [1] (this drawing is also available at the web page `http://www1.mate.polimi.it/~gazzola/modesTNB.pdf`), where an inventory of the modes of oscillation seen at the Tacoma Bridge is drawn.

Since two zeros are always present in the piers, it is necessary to make this precise. First, it is clear that the C^∞-eigenfunctions $\mathbf{O}_\lambda$ and $\mathbf{E}_\lambda$ cannot have double zeros in any point of $\overline{I}$. On the other hand, using the explicit expression of $\mathscr{O}_\lambda$ (resp., $\mathscr{E}_\lambda$), it turns out that $x \in I_0$ is a double zero if and only if

$$\frac{\sin(\lambda x)}{\sinh(\lambda x)} = \frac{\cos(\lambda x)}{\cosh(\lambda x)} = \frac{\sin(\lambda a \pi)}{\sinh(\lambda a \pi)} \quad \left(\text{resp.}, -\frac{\sin(\lambda x)}{\sinh(\lambda x)} = \frac{\cos(\lambda x)}{\cosh(\lambda x)} = \frac{\cos(\lambda a \pi)}{\cosh(\lambda a \pi)} \right). \tag{3.11}$$

Since

$$\left(\frac{\sin(\lambda x)}{\sinh(\lambda x)} \right)' = 0 \quad \text{iff} \quad \frac{\sin(\lambda x)}{\sinh(\lambda x)} = \frac{\cos(\lambda x)}{\cosh(\lambda x)}, \qquad \left(\frac{\cos(\lambda x)}{\cosh(\lambda x)} \right)' = 0 \quad \text{iff} \quad -\frac{\sin(\lambda x)}{\sinh(\lambda x)} = \frac{\cos(\lambda x)}{\cosh(\lambda x)},$$

condition (3.11) may be satisfied only in correspondence of the local minima (or maxima) of the function $\xi(x) = \sin(\lambda x)/\sinh(\lambda x)$ (resp., $\xi(x) = \cos(\lambda x)/\cosh(\lambda x)$). Labeling these stationary points in increasing order as x_k, $k = 1, 2, \ldots$, one sees that $k \mapsto |\xi(x_k)|$ is strictly decreasing. Consequently, (3.11) can be fulfilled only if $x = a\pi$, that is, if the double zero is located at one pier. In a similar way one can reason for the lateral spans, obtaining the following result.

Proposition 9. *Let e_λ be an eigenfunction of problem (3.2). Then e_λ cannot have double zeros elsewhere than at the piers.*

If the eigenfunction has a double zero at the piers, its restriction to the central span is clamped, while its restrictions to the side spans are partially hinged and partially clamped. Corollary 7 provides an example ($a = 1/2$) where the eigenfunctions $\mathscr{O}_\lambda$ of (3.2) have this feature, but no zeros of order greater than 2 are placed in the piers; in fact, the third derivative is therein defined - with nonzero value - only for the C^∞-eigenfunctions $\mathbf{O}_\lambda$ and $\mathbf{E}_\lambda$. We thus define the number of "effective" zeros of an eigenfunction e_λ in I by

$$i(e_\lambda) = \begin{cases} \#\{x \in I_- \cup I_0 \cup I_+ \mid e_\lambda(x) = 0\} & \text{if } e'_\lambda(a\pi) \neq 0 \\ \#\{x \in I_- \cup I_0 \cup I_+ \mid e_\lambda(x) = 0\} + 2 & \text{if } e'_\lambda(a\pi) = 0. \end{cases}$$

Hence, if e_λ possesses double zeros at the piers, then we count them as two additional simple zeros.

The second result of this section gives a complete description of the placement of the zeros of the eigenfunctions; we postpone its lengthy proof to Section 5.5. In order to give the statement, fixed $a \in (0, 1)$ we underline the dependence of the eigenfunctions on a, denoting e_n by $e_{\lambda_n(a)}$, $n = 0, 1, 2, \ldots$

Theorem 10. *For $a \in (0, 1)$, it holds that $i(e_{\lambda_n(a)}) = n$, for every $n = 0, 1, 2, \ldots$. Fixed an integer $n \geqslant 0$, on decreasing of a the zeros of $e_{\lambda_n(a)}$ move by couples from the central span to the side spans whenever the curve $\lambda = \lambda_n(a)$ intersects one of the hyperbolas $\{\lambda = \Lambda_k/a\}$ in the (a, λ)-plane, for some integer $k \geqslant 0$ having the same parity as n.*

By looking at Figure 10, we see that the hyperbolas $\{\lambda = \Lambda_k/a\}$ describe a countable set of lines, each of which intersects the countable set of curves representing the eigenvalues in a countable number of points. Therefore, double zeros in the piers are possible only for a countable set of values of $a < 1$, that is,

for almost every $0 < a < 1$ all the eigenfunctions have simple zeros in the piers.

Theorem 10 states that a double zero is placed in a pier (and by symmetry also in the other one) each time that the curve $(a, \lambda_n(a))$ crosses the graph of one of the hyperbolas $\{\lambda = \Lambda_k/a\}$ (with k having the same parity as n). From there on, proceeding in the direction of decreasing a, the zeros of $e_{\lambda_n(a)}$ move from I_0 to I_+ (and I_-); for any odd n and for a sufficiently small such that $\lambda_n(a)$ lies below the hyperbola $\{\lambda = \Lambda_1/a\}$, all the zeros of $e_{\lambda_n(a)}$ lie in the lateral spans, except for the zero in the origin. For even n, the threshold becomes $\lambda_n(a) < \Lambda_0/a$ and no zeros of $e_{\lambda_n(a)}$ at all belong to I_0 below this threshold. We represent this pattern for some odd eigenfunctions in Figure 10, where the numbers (α, β) in parentheses denote, respectively, the number of zeros of the eigenfunction in $(0, a\pi)$ and in $(a\pi, \pi)$. The sum $\alpha + \beta$ is constant on each branch.

We conclude this section with a curiosity regarding the asymptotic behavior of the eigenvalues, which will be proved in Section 5.6.

Theorem 11. *For every $a \in (0, 1)$, any interval of width 3 contains at least three values of λ for which $\mu = \lambda^4$ is an eigenvalue of (3.2). As a consequence,*

$$\lim_{n \to +\infty} \frac{\lambda_{n+1}(a)}{\lambda_n(a)} = 1 \qquad \forall a \in (0, 1). \tag{3.12}$$

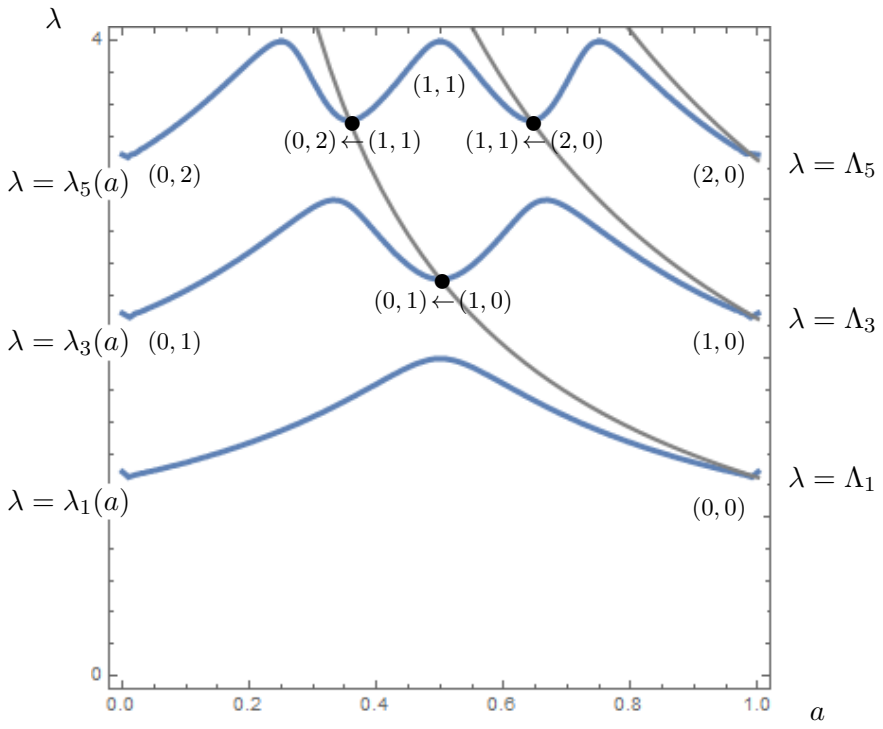

Figure 10: A visual description of Theorem 10 for the curves $\lambda = \lambda_{2m+1}(a)$.

3.3 Plots of some particular eigenfunctions

In this section, we focus on some given values of a, for which the eigenvalues are determined numerically, and we plot some pictures of eigenfunctions. In particular, we consider the cases $a = 14/25$ (the ratio of the spans of the Tacoma Bridge, according to [1]) and $a = 1/2$ portraited, respectively, in Figures 11 and 12. In all the plots, the dot $\bullet$ represents the position of the piers. We recall that for $a = 1/2$ there are eigenfunctions with double zeros in the piers, as stated in Corollary 7.

In Table 1 we quote the eigenvalues relative to the eigenfunctions plotted in Figures 11 and 12.

a	μ_0	μ_1	μ_2	μ_3	μ_4	μ_5	μ_6	μ_7	μ_8	μ_9	μ_{10}	μ_{11}
14/25	1.74	13.8	35.5	47.3	84	205	409	533	633	1004	1684	2347
1/2	2.44	16	25.6	39	112	256	326	410	760	1296	1526	1785

Table 1: The least 12 eigenvalues of (3.1) for $a = 14/25$ and $a = 1/2$, with an approximation of 1%.

The possibility of having double zeros in the piers naturally leads to wonder whether positive eigenfunctions may exist, namely $e_\lambda(x) > 0$ for every $x \in I_- \cup I_0 \cup I_+$. Of course, this can happen only for an even eigenfunction. Moreover, by Proposition 9 the only possibility is to have double zeros in the piers, since otherwise the eigenfunction would change sign crossing the piers. Due to the nodal properties of the eigenfunctions stated in Theorem 10, this means that the only eigenfunction that can be positive is the third one. Denoting by $\mu_2(a) = \lambda_2^4(a)$ the third eigenvalue, we are thus led to seek the value of a such that $\lambda_2(a) = \Lambda_0/a$, where $\mu = \Lambda_0^4$ is the least eigenvalue of (3.6). We numerically find that

if $a \approx 0.3759$, then $\mu_2 \approx 16.0863$ ($\lambda_2 \approx 2.00269$) and the third eigenfunction is positive; this is the only choice of (a, λ) for which an eigenfunction of (3.2) is positive.

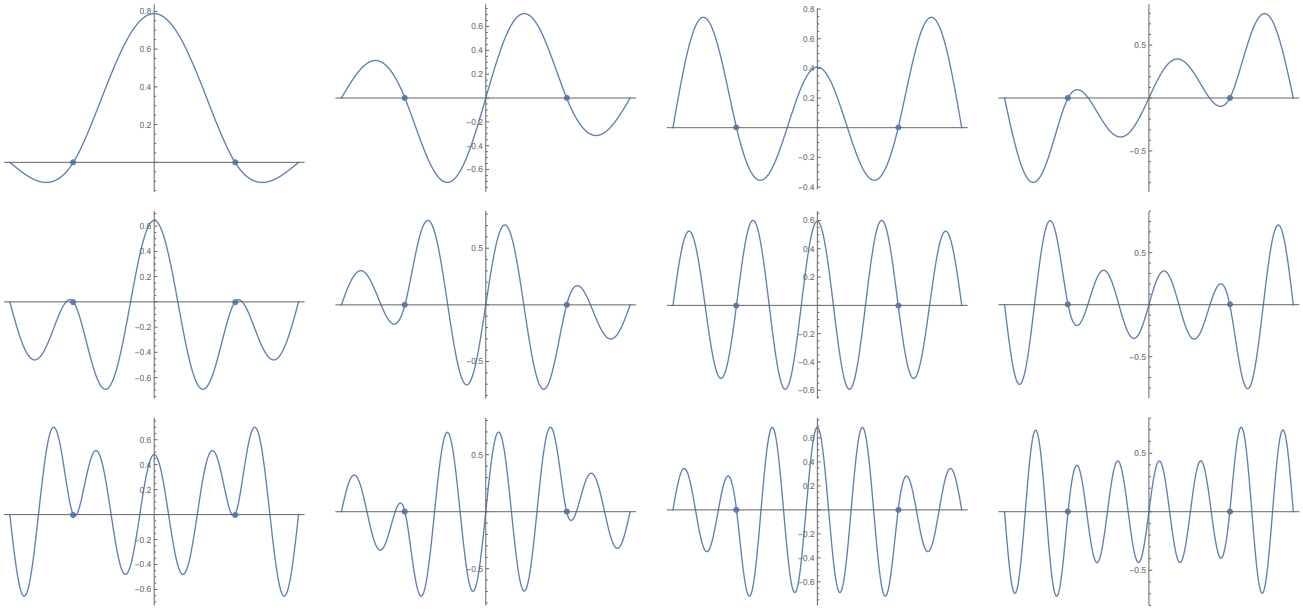

Figure 11: The first twelve L^2-normalized eigenfunctions of (3.1) when $a = 14/25$.

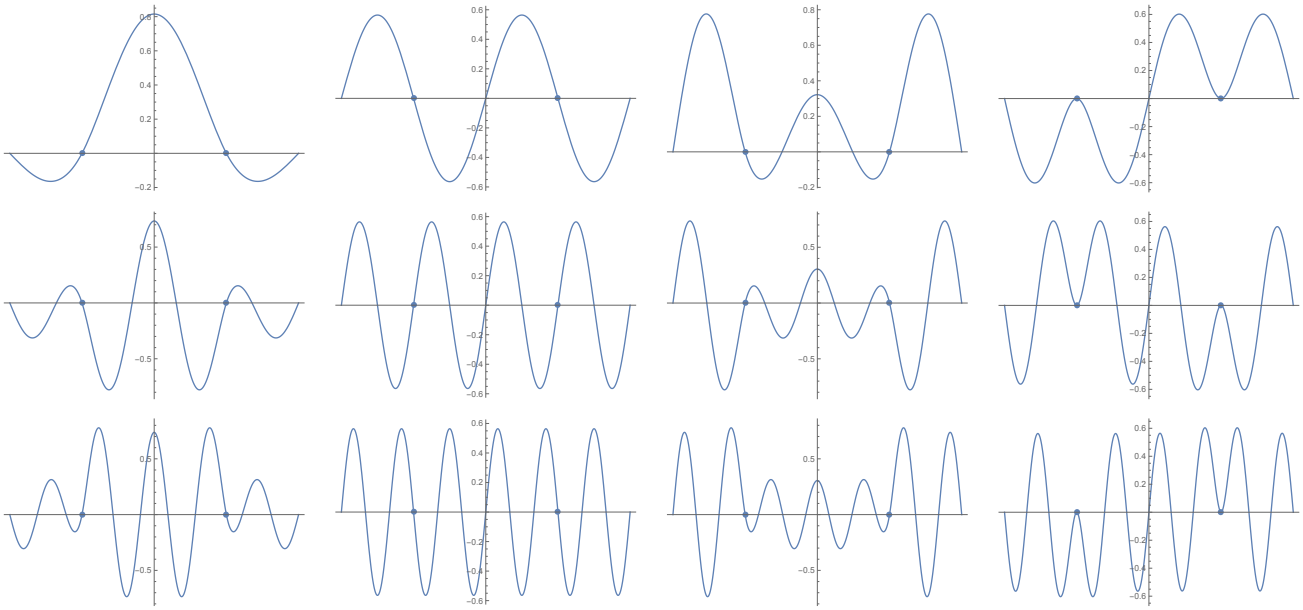

Figure 12: The first twelve L^2-normalized eigenfunctions of (3.1) when $a = 1/2$.

In Figure 13, we plot the shape of the third eigenfunction e_2 on varying of $0 < a < 1$. It can be seen how the global minima of e_2 move when the side spans are enlarged. In particular, for $a \gtrapprox 0.3759$ (resp. $a \lessapprox 0.3759$) the minima are in the central span (resp. lateral spans).

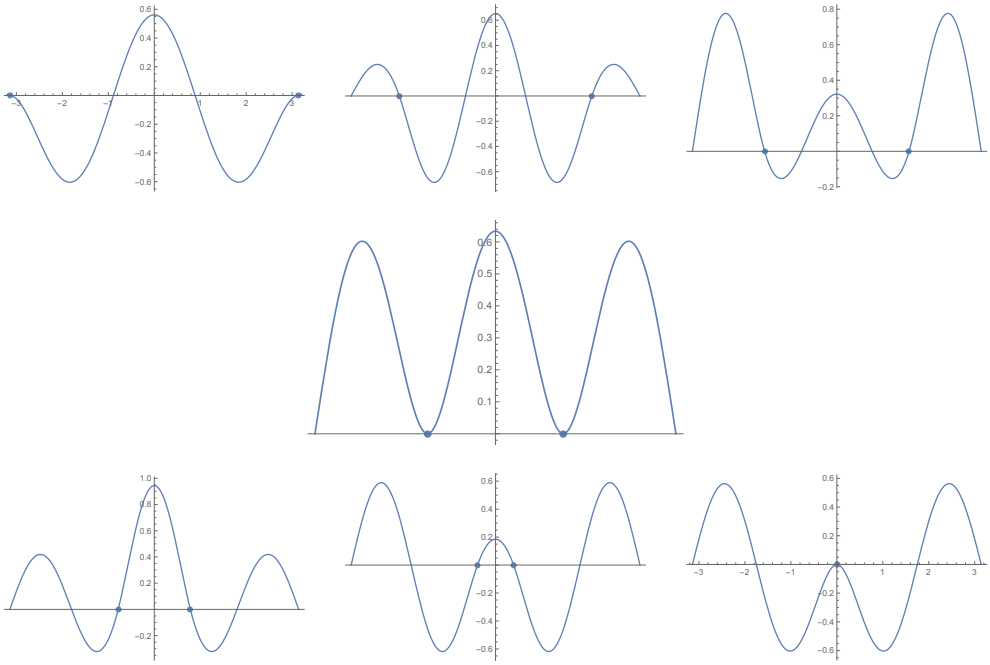

Figure 13: The third eigenfunction e_2 for $a = 1$ (i.e., for the clamped beam), $a = 2/3$, $a = 1/2$ (first line), $a = 0.3759$ (second line), $a = 1/4$, $a = 1/8$, $a = 0$ (third line).

4 A related second order eigenvalue problem

This section is motivated by the observation that the operator L defined on $V(I)$ by $\langle Lu, v\rangle_V = \int_I u''v''$ *is not* the square of the operator $\mathcal{L}$ defined on $W(I)$ by $\langle \mathcal{L}u, v\rangle_W = \int_I u'v'$, where

$$W(I) := \{u \in H_0^1(I);\, u(\pm a\pi) = 0\} \tag{4.1}$$

and $\langle\cdot,\cdot\rangle_W$ denotes the duality pairing between $W'(I)$, the dual space of $W(I)$, and $W(I)$. Notice that, since $W(I) \subset C(I)$, the pointwise constraints still make sense.

We formalize this observation through the following statement.

Proposition 12. *Let $a \in (0,1)$ and let e_λ be an eigenfunction of (3.2) with associated eigenvalue $\mu = \lambda^4$. Then*

$$\Upsilon_\lambda^2 := \frac{\int_I (e_\lambda')^2}{\int_I e_\lambda^2} \begin{cases} = \lambda^2 & \text{if } e_\lambda \in C^\infty(I) \\ < \lambda^2 & \text{otherwise.} \end{cases} \tag{4.2}$$

The proof of Proposition 12 is obtained in two steps. First, the inequality $\Upsilon_\lambda \leqslant \lambda$ follows from an integration by parts and from the Hölder inequality:

$$\int_I (e_\lambda')^2 \leqslant \int_I |e_\lambda e_\lambda''| \leqslant \left(\int_I e_\lambda^2\right)^{1/2} \left(\int_I (e_\lambda'')^2\right)^{1/2} = \lambda^2 \int_I e_\lambda^2.$$

Then, this inequality is an equality if and only if e_λ and e_λ'' are proportional and, according to Theorem 6, this happens if and only if $e_\lambda \in C^\infty(I)$.

The number Υ_λ in (4.2) may be seen as a "correction term" due to the presence of the piers and highlights a striking difference compared with the beam without piers, for which $\Upsilon_\lambda = \lambda$ for all λ. Because of Υ_λ, there is no coincidence between the eigenvalues of (3.1) and the squares of the ones of

$$\int_I e'w' = \mu \int_I ew \qquad \forall w \in W(I). \tag{4.3}$$

We provide some spectral results also for (4.3), giving their proof in Section 5.7.

Theorem 13. *The eigenvalues $\mu = \kappa^2$ of problem (4.3) are completely determined by the numbers $\kappa > 0$ such that*

$$(i) \quad \sin(\kappa a\pi)\sin[\kappa(1-a)\pi] = 0 \quad \text{or} \quad (ii) \quad \cos(\kappa a\pi)\sin[\kappa(1-a)\pi] = 0,$$

that is,

$$(i) \quad \kappa \in \frac{\mathbb{N}}{a} \cup \frac{\mathbb{N}}{1-a} \quad \text{or} \quad (ii) \quad \kappa \in \frac{2\mathbb{N}+1}{2a} \cup \frac{\mathbb{N}}{1-a}. \tag{4.4}$$

• *If $\kappa \notin \mathbb{N}/(1-a)$, denoting by χ_0 the characteristic function of I_0, then:*
- in case (i), $\mu = \kappa^2$ is a simple eigenvalue associated with the odd eigenfunction $\mathbf{D}_\kappa(x) = \chi_0(x)\sin(\kappa x)$;
- in case (ii), $\mu = \kappa^2$ is a simple eigenvalue associated with the even eigenfunction $\mathbf{P}_\kappa(x) = \chi_0(x)\cos(\kappa x)$.
• *If $\kappa \in \mathbb{N}/(1-a)$, then the following situations may occur:*
- if $\kappa \notin \mathbb{N}/a$ and $\kappa \notin (2\mathbb{N}+1)/2a$, then $\mu = \kappa^2$ is a double eigenvalue associated with the eigenfunctions

$$\mathcal{D}_\kappa(x) = \begin{cases} \sin[\kappa(x+\pi)] & \text{if } x \in \overline{I}_- \\ 0 & \text{if } x \in \overline{I}_0 \\ \sin[\kappa(x-\pi)] & \text{if } x \in \overline{I}_+, \end{cases} \qquad \mathcal{P}_\kappa(x) = \begin{cases} \sin[\kappa(x+\pi)] & \text{if } x \in \overline{I}_- \\ 0 & \text{if } x \in \overline{I}_0 \\ \sin[\kappa(\pi-x)] & \text{if } x \in \overline{I}_+, \end{cases}$$

respectively odd and even;
- if $\kappa \in \mathbb{N}/a$, then $\mu = \kappa^2$ is a triple eigenvalue associated with $\mathcal{D}_\kappa$, $\mathcal{P}_\kappa$ and $\mathbf{D}_\kappa$;
- if $\kappa \in (2\mathbb{N}+1)/2a$, then $\mu = \kappa^2$ is a triple eigenvalue associated with $\mathcal{D}_\kappa$, $\mathcal{P}_\kappa$ and $\mathbf{P}_\kappa$.

Notice that (4.4)-(i) corresponds to odd eigenfunctions, while (4.4)-(ii) to even ones. The eigenfunctions of (4.3) are obtained by juxtaposing the eigenfunctions belonging to H_0^1 of each span, since there are no smooth junction constraints; for this reason, in general they are not C^1. It is also worthwhile noticing that the eigenvalues may be both simple or multiple. Simple eigenvalues are always associated with eigenfunctions being zero on the side spans. Multiple eigenfunctions exist when $\kappa \in \mathbb{N}/(1-a)$ and, in this case, the choice of the associated eigenfunctions is quite arbitrary. In the case of a double eigenvalue, we have chosen to maintain the distinction between odd and even generators, as in Theorem 6. For triple eigenvalues, we chose to separate the behavior on the central span from the one on the two side spans, at the price of losing regularity. Indeed, in this case C^∞-eigenfunctions exist and coincide with $\mathbf{O}_\lambda$ and $\mathbf{E}_\lambda$ appearing in Theorem 6, but associated with the eigenvalue $\mu = \lambda^2$: for the eigenvalues $\mu = \lambda^4$ of (3.2) associated with $\mathbf{O}_\lambda$ and $\mathbf{E}_\lambda$ one has in fact $\Upsilon_\lambda = \lambda$, see (4.2). Observe that there are no triple eigenvalues if $a \notin \mathbb{Q}$.

This choice of the eigenfunctions is motivated by the possibility of analyzing separately the behavior on the central span, that is the most vulnerable part in bridges. Other equivalent bases are possible: for instance, one could replace $\mathcal{D}_\kappa$ and $\mathcal{P}_\kappa$ by the functions having only one nontrivial component on I_- and I_+, respectively. In Figure 14 we depict the curves of eigenvalues in the plane (a, κ): the bold hyperbolas correspond to $\kappa \in \mathbb{N}/(1-a)$, the dashed lines to $\kappa \in (2\mathbb{N}+1)/2a$ and the dot-dashed ones to $\kappa \in \mathbb{N}/a$.

We now provide a formula which identifies simple, double and triple eigenvalues. To this purpose, we introduce the real sequence $\{\omega_n\}_n$ defined by

$$\omega_n = \frac{n+1}{n+3}, \qquad n \geqslant -1,$$

so that $\omega_n \to 1$ for $n \to +\infty$ and the first ω_n's are equal to $0, \frac{1}{3}, \frac{1}{2}, \frac{3}{5}, \frac{2}{3}$. We have the following statement, which can be proved by noticing that the simple eigenvalues of (4.3) are given by the numbers $n/2a$, $n \in \mathbb{N}$.

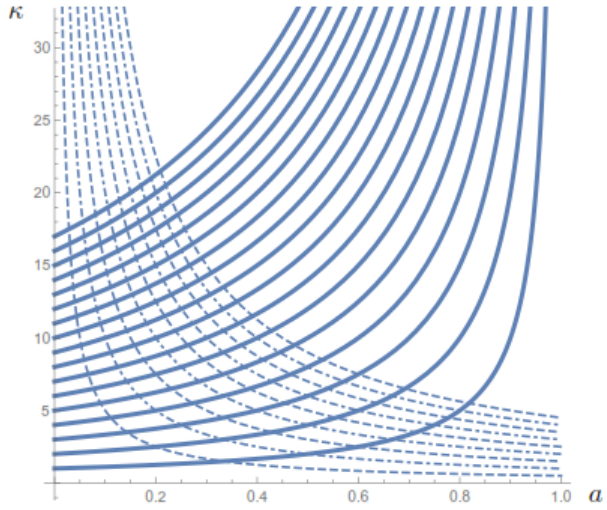

Figure 14: A pictorial description of the curves of eigenvalues for (4.3), in the (a, κ)-plane.

Proposition 14. *The following facts hold:*
• *if* $\omega_{n-1} < a \leqslant \omega_n$, *then the first* n *eigenvalues of* (4.3) *are simple* ($n \geqslant 0$); *moreover, if* $a = \omega_n$, *then the* $(n+1)$*-th eigenvalue is triple;*
• *if* $\frac{1}{2m+3} \leqslant a < \frac{1}{2m+1}$, *then the first* m *eigenvalues of* (4.3) *are double, with an odd and an even eigenfunction* ($m \geqslant 0$); *moreover, if* $a = \frac{1}{2m+3}$, *then the* $(m+1)$*-th eigenvalue is triple.*

In particular, we infer that the first eigenvalue is simple for $a > 1/3$, triple for $a = 1/3$, double for $a < 1/3$. Moreover, the second eigenvalue is simple for $a > 1/2$ and triple for $a = 1/2$. Overall, Proposition 14 states that the multiplicity increases on low eigenvalues when a is small.

Each bold hyperbola in Figure 14 carries a double eigenvalue, with one even and one odd eigenfunction, while each of the dashed and dot-dashed hyperbolas therein carries a simple eigenvalue, alternating even and odd eigenfunctions. In Figures 15 and 16 we depict the shape of the first ten/twelve eigenfunctions for $a = 1/2 = \omega_1$ and $a = 14/25 \in (\omega_1, \omega_2)$, and in Table 2 we quote the corresponding eigenvalues: in case of multiple eigenvalues we plot first $\mathbf{D}_\kappa$ or $\mathbf{P}_\kappa$ (if they exist), then $\mathcal{D}_\kappa$, finally $\mathcal{P}_\kappa$.

a	μ_0	μ_1	μ_2	μ_3	μ_4	μ_5	μ_6	μ_7	μ_8	μ_9
14/25	0.797194	3.18876	5.1653	5.1653	7.17474	12.7551	19.9299	20.6611	20.6611	28.6989
1/2	1	4	4	4	9	16	16	16	25	36

Table 2: The least ten eigenvalues of (4.3) for $a = 14/25$ and $a = 1/2$.

5 Proofs

5.1 Proof of Theorem 3

Existence and uniqueness of the weak solution $u \in V(I)$ follow directly from the Lax-Milgram Theorem, since $\gamma \geqslant 0$.

(i) By arguing as in [8, Lemma 2.2] and performing an integration by parts similar to that in [10, Example 1] in the final part, we find that a weak solution u of (2.6)-(2.2) belongs to $C^2(I)$ and is of

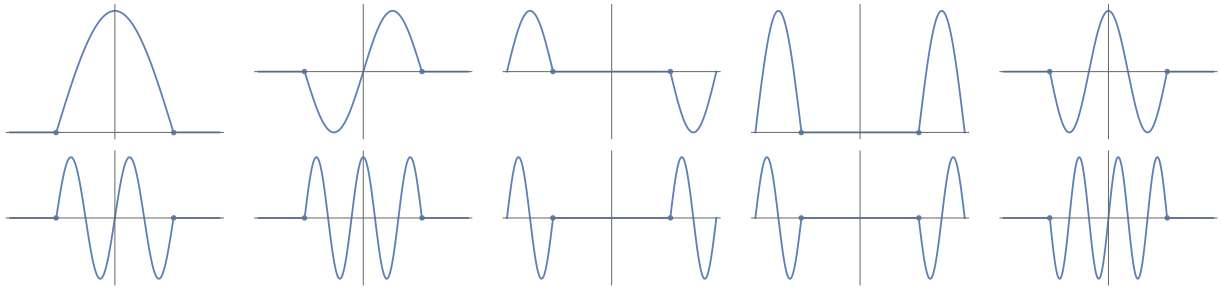

Figure 15: The shape of the first ten eigenfunctions of (4.3) when $a = 14/25$.

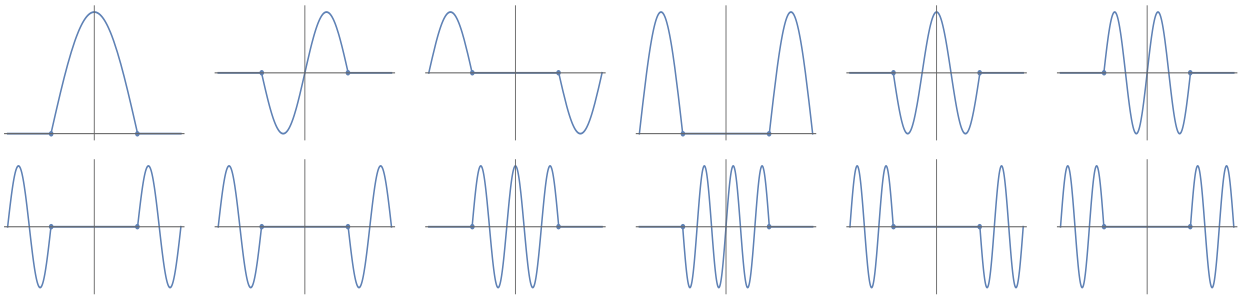

Figure 16: The shape of the first twelve eigenfunctions of (4.3) when $a = 1/2$.

class C^4 on each subinterval $\overline{I}_-$, $\overline{I}_0$ and $\overline{I}_+$. Moreover, by performing two integration by parts on each subinterval, the terms computed in $-b\pi, a\pi$ compensate (due to the C^2-regularity); Definition 2 is then fulfilled only if $u''(\pm\pi) = 0$, due to the arbitrariness of $v \in V(I)$.

(ii) In order to prove this statement, we introduce a general procedure for the analysis of (2.6) that we first describe in detail in the case $\gamma = 0$. Let $f \in C^0(\overline{I})$ and consider the classical solution U_f of the problem

$$U_f''''(x) = f(x) \qquad x \in I, \qquad U_f(-\pi) = U_f(-b\pi) = U_f(a\pi) = U_f(\pi) = 0.$$

Clearly, $U_f \in C^4(\overline{I}) \cap V(I)$ but U_f may not be a weak solution (according to Definition 2) because it may fail to fulfill the conditions $U_f''(-\pi) = U_f''(\pi) = 0$ required by the just proved Item (i). Wishing to satisfy (2.8), we add to U_f three third order polynomials P_b, P_0, P_a defined, respectively, in $[-\pi, -b\pi]$, $[-b\pi, a\pi]$, $[a\pi, \pi]$, satisfying

$$\begin{gathered} P_b(x)=(x+\pi)(x+b\pi)(Ax+B\pi),\ P_0(x)=(x+b\pi)(x-a\pi)(Cx+D\pi),\ P_a(x)=(x-a\pi)(x-\pi)(Ex+F\pi), \\ P_b'(-b\pi)=P_0'(-b\pi), \quad P_b''(-b\pi)=P_0''(-b\pi), \quad P_a'(a\pi)=P_0'(a\pi), \quad P_a''(a\pi)=P_0''(a\pi). \end{gathered} \tag{5.1}$$

The first line in (5.1) guarantees that these polynomials vanish at the endpoints of the interval where they are defined, whereas the second line in (5.1) ensures that they match C^2 in $\{-b\pi, a\pi\}$. Then we introduce two further constraints of no bending at the endpoints, that is,

$$P_b''(-\pi) = -U_f''(-\pi) =: f_b, \qquad P_a''(\pi) = -U_f''(\pi) =: f_a. \tag{5.2}$$

The first line in (5.1) introduces six unknowns A, B, C, D, E, F, to be determined. The second line in (5.1) gives four equations, whereas (5.2) gives two further equations, all being linear and linking the six unknowns. The former four conditions are "structural" since they only depend on a and b, while the two latter conditions are "forced" since they also depend on the source f through the function U_f.

Since these six equations are linearly independent, they uniquely determine the unknowns A, B, C, D, E, F. Take these constants and replace them into the polynomials in (5.1). Then the solution of (2.8) has the form

$$u(x) = U_f(x) + \begin{cases} P_b(x) & \text{if } x \in [-\pi, -b\pi] \\ P_0(x) & \text{if } x \in [-b\pi, a\pi] \\ P_a(x) & \text{if } x \in [a\pi, \pi]. \end{cases} \tag{5.3}$$

Next, we analyze the possible discontinuities of the third derivative of this weak solution. In view of (5.1) and (5.3), we have

$$\begin{aligned} u'''(-b\pi^+) - u'''(-b\pi^-) = P_0'''(-b\pi) - P_b'''(-b\pi) = 6(C - A) =: \beta_f, \\ u'''(a\pi^+) - u'''(a\pi^-) = P_a'''(a\pi) - P_0'''(a\pi) = 6(E - C) =: \alpha_f. \end{aligned} \tag{5.4}$$

Therefore, we may rewrite (2.6) with $\gamma = 0$ in the following distributional form:

$$u'''' = f + \beta_f \delta_{-b\pi} + \alpha_f \delta_{a\pi}, \tag{5.5}$$

which completes the proof of Item (ii) in the case $\gamma = 0$.

If $\gamma = 4\nu^4 > 0$, consider the classical solution U_f of the problem

$$U_f''''(x) + 4\nu^4 U_f(x) = f(x) \qquad x \in I, \qquad U_f(-\pi) = U_f(-b\pi) = U_f(a\pi) = U_f(\pi) = 0. \tag{5.6}$$

Such a solution exists and is unique: one may fulfill the four-point conditions in (5.6) by adding to any solution of the differential equation in (5.6) a suitable linear combination of the functions in

$$K := \Big\{ \cos(\nu x)\cosh(\nu x),\, \cos(\nu x)\sinh(\nu x),\, \sin(\nu x)\cosh(\nu x),\, \sin(\nu x)\sinh(\nu x) \Big\},$$

which generate the 4-dimensional kernel of the operator $w \mapsto w'''' + 4\nu^4 w$. Again, U_f may not be a weak solution and, in order to satisfy (2.8), we seek three linear combinations of the functions in K, that we call P_b, P_0, P_a, defined respectively in $\overline{I}_-$, $\overline{I}_0$, $\overline{I}_+$, and satisfying the conditions

$$\begin{gathered} P_b(-\pi) = P_b(-b\pi) = 0,\ P_0(-b\pi) = P_0(a\pi) = 0,\ P_a(a\pi) = P_a(\pi) = 0, \\ P_b'(-b\pi) = P_0'(-b\pi), \quad P_b''(-b\pi) = P_0''(-b\pi), \quad P_a'(a\pi) = P_0'(a\pi), \quad P_a''(a\pi) = P_0''(a\pi), \\ P_b''(-\pi) = -U_f''(-\pi), \quad P_a''(\pi) = -U_f''(\pi). \end{gathered} \tag{5.7}$$

The first line in (5.7) guarantees that these combinations vanish at the endpoints of the interval where they are defined. The second line in (5.7) ensures that they match C^2 in $\{-b\pi, a\pi\}$. The third line in (5.7) forces the solution to have no bending at the endpoints, in line with Item (i). Overall, (5.7) contains twelve conditions. There are also twelve unknowns: the four coefficients of the linear combinations of the elements in K, for each of the three functions P_b, P_0, P_a. One finds these unknowns by solving the corresponding linear system and the weak solution of (2.8) is again given by (5.3). The same arguments used for (5.4) and (5.5) lead to the distributional equation $u'''' + 4\nu^4 u = f + \beta_f \delta_{-b\pi} + \alpha_f \delta_{a\pi}$. This completes the proof of Item (ii) also for $\gamma > 0$.

(iii) The subspace $X(I) \subset C^0(\overline{I})$ is defined by the two (linear) constraints $\beta_f = \alpha_f = 0$.

(iv) In view of (5.4), we have $u \in C^3(\overline{I})$ if and only if $\beta_f = \alpha_f = 0$ which, by the just proved Item (iii), yields $u \in C^4(\overline{I})$.

5.2 Proof of Theorem 5

Since $e(x)$ is of class C^4 on $\overline{I}_-, \overline{I}_0$ and $\overline{I}_+$ in view of Theorem 3, we can write

$$e(x) = \begin{cases} e_b(x) & \text{if } x \in [-\pi, -b\pi] \\ e_0(x) & \text{if } x \in [-b\pi, a\pi] \\ e_a(x) & \text{if } x \in [a\pi, \pi], \end{cases} \tag{5.8}$$

where e_b, e_0 and e_a are classical solutions of $e'''' = \lambda^4 e$ on their intervals of definition. Consequently, on each span, $e(x)$ is a linear combination of the four functions

$$\cos(\lambda x), \quad \sin(\lambda x), \quad \cosh(\lambda x), \quad \sinh(\lambda x). \tag{5.9}$$

We thus seek the coefficients of all the nonzero linear combinations of (5.9) for which $e(x)$ as in (5.8) is a solution of (3.2).

By imposing that $e_b(-\pi) = e_b''(-\pi) = e_b(-b\pi) = 0$, one finds that ($K_b \in \mathbb{R}$)

$$e_b(x) = K_b \Big\{ \sinh\big[\lambda(1-b)\pi\big] \sin\big[\lambda(x+\pi)\big] - \sin\big[\lambda(1-b)\pi\big] \sinh\big[\lambda(x+\pi)\big] \Big\}.$$

By imposing that $e_a(\pi) = e_a''(\pi) = e_a(a\pi) = 0$, one finds that ($K_a \in \mathbb{R}$)

$$e_a(x) = K_a \Big\{ \sinh\big[\lambda(1-a)\pi\big] \sin\big[\lambda(x-\pi)\big] - \sin\big[\lambda(1-a)\pi\big] \sinh\big[\lambda(x-\pi)\big] \Big\}.$$

Finally, by requiring that $e_0(-b\pi) = e_0(a\pi) = 0$ one deduces that ($K_1, K_2 \in \mathbb{R}$)

$$\begin{aligned} e_0(x) \;=\; & K_1 \Big\{ \sinh\big[\lambda(a+b)\pi\big] \cos(\lambda x) + \cos(\lambda b\pi) \sinh\big[\lambda(x-a\pi)\big] - \cos(\lambda a\pi) \sinh\big[\lambda(x+b\pi)\big] \Big\} \\ & + K_2 \Big\{ \sinh\big[\lambda(a+b)\pi\big] \sin(\lambda x) - \sin(\lambda b\pi) \sinh\big[\lambda(x-a\pi)\big] - \sin(\lambda a\pi) \sinh\big[\lambda(x+b\pi)\big] \Big\}. \end{aligned}$$

Then (3.2) is satisfied if and only if these functions match C^2 in $-b\pi$ and in $a\pi$, so that the eigenfunction e in (5.8) belongs to $C^2(\overline{I})$. This leads to a 4×4 linear system of K_b, K_a, K_1, K_2, and nontrivial solutions are obtained by imposing that the determinant of such system is equal to 0. This requirement is precisely the condition in the statement.

5.3 Proof of Theorem 6

Thanks to the symmetry of the interval I, we can seek odd and even eigenfunctions of (3.2) separately. Moreover, we can restrict our attention to the half-interval $[0, \pi]$, aiming at determining e_0, e_a such that

$$e(x) = \begin{cases} e_0(x) & \text{if } x \in [0, a\pi] \\ e_a(x) & \text{if } x \in [a\pi, \pi] \end{cases} \tag{5.10}$$

solves (3.2) (recall (5.8)); the expression of e over $[-\pi, 0]$ is then obtained by prolonging (5.10) by symmetry, either even or odd. Following this scheme, we only have to impose the C^2-matching of the functions e_0 and e_a in $x = a\pi$.

Using the same notation as in the proof of Theorem 5, when searching for odd solutions this leads to set $K_1 = 0$ and results into the system

$$\begin{cases} (\cos[\lambda(1-a)\pi]\sinh[\lambda(1-a)\pi] - \sin[\lambda(1-a)\pi]\cosh[\lambda(1-a)\pi])K_a = 2\cosh(\lambda a\pi)(\cos(\lambda a\pi)\sinh(\lambda a\pi) - \sin(\lambda a\pi)\cosh(\lambda a\pi))K_2 \\ \sin[\lambda(1-a)\pi]\sinh[\lambda(1-a)\pi]K_a + 2\sin(\lambda a\pi)\sinh(\lambda a\pi)\cosh(\lambda a\pi)K_2 = 0. \end{cases} \tag{5.11}$$

Nontrivial solutions of this system exist when the associated determinant is equal to zero, namely when (3.3) holds. We distinguish two cases:

- if $\lambda \in \mathbb{N}$, then (3.3) has to hold with both sides equal to 0, so that necessarily $\lambda a \in \mathbb{N}$ and, consequently, also $\lambda(1-a) \in \mathbb{N}$. The second equation in (5.11) is thus identically satisfied, while the first equation reads

$$\cos(\lambda\pi)\sinh[\lambda(1-a)\pi]K_a = 2\cosh(\lambda a\pi)\sinh(\lambda a\pi)K_2$$

(recall that $\sin(\lambda a\pi) = 0$, so that $|\cos(\lambda a\pi)| = 1$). This yields the eigenfunction $\mathbf{O}_\lambda = \sin(\lambda x)$ for the choices $K_a = \frac{1}{\cos(\lambda\pi)\sinh[\lambda(1-a)\pi]}$, $K_2 = \frac{1}{2\cosh(\lambda a\pi)\sinh(\lambda a\pi)}$;

- if $\lambda \notin \mathbb{N}$, then by (3.3) it is necessarily $\lambda a \notin \mathbb{N}$ and $\lambda(1-a) \notin \mathbb{N}$. The explicit form of $\mathscr{O}_\lambda$ can then be derived by using the second equation of system (5.11), choosing $K_a = -\frac{\sin(\lambda a\pi)}{\sin[\lambda(1-a)\pi]}$ and $K_2 = \frac{\sinh[\lambda(1-a)\pi]}{2\cosh(\lambda a\pi)\sinh(\lambda a\pi)}$.

This completes the proof for odd eigenfunctions.

Similarly, the search for even solutions leads to set $K_2 = 0$ and results into the system

$$\begin{cases} (\sin[\lambda(1-a)\pi]\cosh[\lambda(1-a)\pi] - \cos[\lambda(1-a)\pi]\sinh[\lambda(1-a)\pi])K_a = 2\sinh(\lambda a\pi)(\cos(\lambda a\pi)\sinh(\lambda a\pi) + \sin(\lambda a\pi)\cosh(\lambda a\pi))K_1 \\ \sin[\lambda(1-a)\pi]\sinh[\lambda(1-a)\pi]K_a + 2\cos(\lambda a\pi)\sinh(\lambda a\pi)\cosh(\lambda a\pi)K_1 = 0. \end{cases}$$

The proof is here analogous to the one for odd eigenfunctions: the determinant associated with the system is equal to zero if and only if (3.4) holds, and a similar analysis to the one performed above yields the result.

5.4 Proof of Theorem 8

The linear operator L defined on $V(I)$ by $\langle Lu, v\rangle_V = \int_I u''v''$ is self-adjoint. Hence, its eigenfunctions form a basis of $V(I)$. For the rest of the proof, it is convenient to make a change of variables. We set $\Lambda = \lambda a$ and $\alpha = 1/a$, so that $\alpha \in (1, +\infty)$ and the eigenvalue problem (3.1) is rephrased as

$$\int_J e''v'' = \mu \int_J ev \qquad \forall v \in V(J), \tag{5.12}$$

being $J = (-\alpha\pi, \alpha\pi)$, $\overline{J} = \overline{J}_- \cup \overline{J}_0 \cup \overline{J}_+$, with $\overline{J}_- = [-\alpha\pi, -\pi]$, $\overline{J}_0 = [-\pi, \pi]$ and $\overline{J}_+ = [\pi, \alpha\pi]$, and $V(J) = \{u \in H^2 \cap H_0^1(J);\, u(-\pi) = u(\pi) = 0\}$. With this procedure, we view the piers as fixed in $\pm\pi$ and move the endpoints $\pm\alpha\pi$ of the beam. Accordingly, (3.3) and (3.4) are changed, respectively, into

$$\sin(\Lambda\alpha\pi)\sinh(\Lambda\pi)\sinh[\Lambda(\alpha-1)\pi] = \sinh(\Lambda\alpha\pi)\sin(\Lambda\pi)\sin[\Lambda(\alpha-1)\pi] \tag{5.13}$$

$$\cos(\Lambda\alpha\pi)\cosh(\Lambda\pi)\sinh[\Lambda(\alpha-1)\pi] = \cosh(\Lambda\alpha\pi)\cos(\Lambda\pi)\sin[\Lambda(\alpha-1)\pi], \tag{5.14}$$

and the corresponding eigenfunctions $\mathscr{O}_\Lambda$ and $\mathscr{E}_\Lambda$ are given, respectively, by the odd and the even extensions of

$$\mathscr{O}_\lambda(x) = \begin{cases} \dfrac{\sinh[\Lambda(\alpha-1)\pi]}{\sinh(\Lambda\pi)}\left(\sinh(\Lambda\pi)\sin(\Lambda x) - \sin(\Lambda\pi)\sinh(\Lambda x)\right) & \text{if } x \in [0,\pi] \\ \dfrac{\sin(\Lambda\pi)}{\sin[\Lambda(\alpha-1)\pi]}\left(\sin[\Lambda(\alpha-1)\pi]\sinh[\Lambda(x-\alpha\pi)] - \sinh[\Lambda(\alpha-1)\pi]\sin[\Lambda(x-\alpha\pi)]\right) & \text{if } x \in [\pi,\alpha\pi], \end{cases}$$

and

$$\mathscr{E}_\lambda(x) = \begin{cases} \dfrac{\sinh[\Lambda(\alpha-1)\pi]}{\cosh(\Lambda\pi)}\left(\cosh(\Lambda\pi)\cos(\Lambda x) - \cos(\Lambda\pi)\cosh(\Lambda x)\right) & \text{if } x \in [0,\pi] \\ \dfrac{\cos(\Lambda\pi)}{\sin[\Lambda(\alpha-1)\pi]}\left(\sinh[\Lambda(\alpha-1)\pi]\sin[\Lambda(\alpha\pi-x)] - \sin[\Lambda(\alpha-1)\pi]\sinh[\Lambda(\alpha\pi-x)]\right) & \text{if } x \in [\pi,\alpha\pi], \end{cases}$$

while $\mathbf{O}_\Lambda$ and $\mathbf{E}_\Lambda$ respectively become equal to $\sin(\Lambda x)$ and $\cos(\Lambda x)$ for $x \in J$. Furthermore, the hyperbolas $\lambda = \Lambda_n/a$ in the (a,λ)-plane become the horizontal lines $\Lambda = \Lambda_n$ in the (α,Λ)-plane, and the curves defining the eigenvalues become strictly decreasing, as we state in the following theorem. This is well depicted in Figures 17 and 18.

The statement that we are going to prove in this new framework is the following.

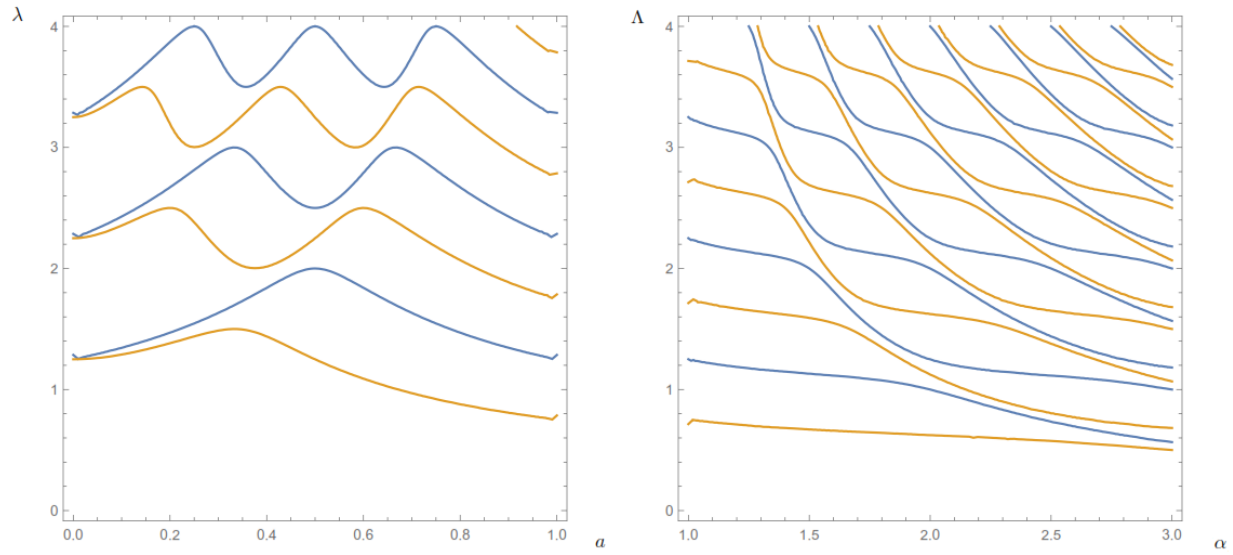

Figure 17: The solutions $\lambda = \lambda(a)$ of (3.3) and (3.4) (left) and $\Lambda = \Lambda(\alpha)$ of (5.13) and (5.14) (right).

Theorem 8'. *For any $\alpha > 1$, the eigenvalues $\mu = \Lambda^4$ of problem* (5.12) *are simple and form a countable set. Moreover,* (5.13) *and* (5.14) *implicitly define, for $\alpha \in (1, +\infty)$, a countable family of analytic and strictly decreasing functions $\alpha \mapsto \Lambda_n(\alpha)$ satisfying $\Lambda_n(\alpha) \to \Lambda_n$ (see* (3.7)*) for $\alpha \to 1$ (n=0, 1, 2, ...).*

The proof of Theorem 8' is based on two lemmas. With the first one, we characterize the eigenvalues of problem (5.12) as functions of α. To this end, we define $I, P : (1, +\infty) \times (0, +\infty) \to \mathbb{R}$ as

$$I(\alpha, \Lambda) = \sin(\Lambda\alpha\pi)\sinh(\Lambda\pi)\sinh[\Lambda(\alpha-1)\pi] - \sinh(\Lambda\alpha\pi)\sin(\Lambda\pi)\sin[\Lambda(\alpha-1)\pi],$$
$$P(\alpha, \Lambda) = \cos(\Lambda\alpha\pi)\cosh(\Lambda\pi)\sinh[\Lambda(\alpha-1)\pi] - \cosh(\Lambda\alpha\pi)\cos(\Lambda\pi)\sin[\Lambda(\alpha-1)\pi].$$

Moreover, we denote by C_I and C_P the 0-level sets of I and P, respectively, and we observe that they are characterized by (5.13) and (5.14). We prove the following result.

Lemma 15. *The equalities $I(\alpha, \Lambda) = 0$ and $P(\alpha, \Lambda) = 0$ implicitly define a family of analytic strictly decreasing functions $\alpha \mapsto \Lambda(\alpha)$ on each connected component of C_I and C_P, respectively.*

Proof. We carry on a detailed proof only for the odd eigenfunctions, since the arguments for the even ones are similar. We set $C_I^0 := C_I \cap \{(\alpha, \Lambda) \mid \Lambda \in \mathbb{N}\}$ and we denote the partial derivatives with respect to Λ and α through the subscripts $_\Lambda$ and $_\alpha$. Since

$$\begin{aligned} I_\alpha(\alpha, \Lambda) \;=\; & \Lambda\pi(\cos(\Lambda\alpha\pi)\sinh(\Lambda\pi)\sinh[\Lambda(\alpha-1)\pi] + \sin(\Lambda\alpha\pi)\sinh(\Lambda\pi)\cosh[\Lambda(\alpha-1)\pi] \\ & - \cosh(\Lambda\alpha\pi)\sin(\Lambda\pi)\sin[\Lambda(\alpha-1)\pi] - \sinh(\Lambda\alpha\pi)\sin(\Lambda\pi)\cos[\Lambda(\alpha-1)\pi]), \end{aligned}$$

noticing that $\Lambda \in \mathbb{N}$ is equivalent to $\Lambda\alpha \in \mathbb{N}$ for the solutions of $I(\alpha, \Lambda) = 0$ we immediately have that

$$I_\alpha\big|_{C_I^0} = \Lambda\pi\cos(\Lambda\alpha\pi)\sinh(\Lambda\pi)\sinh[\Lambda(\alpha-1)\pi], \tag{5.15}$$

while some computations show that

$$I_\alpha\big|_{C_I \setminus C_I^0} = \Lambda\pi\sin(\Lambda\pi)\sinh(\Lambda\pi)\frac{\sin[\Lambda(\alpha-1)\pi]^2 - \sinh[\Lambda(\alpha-1)\pi]^2}{\sin[\Lambda(\alpha-1)\pi]\sinh[\Lambda(\alpha-1)\pi]}. \tag{5.16}$$

On the other hand,

$$I_\Lambda\big|_{C_I^0} = \alpha\pi\cos(\Lambda\alpha\pi)\sinh(\Lambda\pi)\sinh[\Lambda(\alpha-1)\pi], \tag{5.17}$$

and

$$I_\Lambda\big|_{C_I\setminus C_I^0} = \frac{\alpha-1}{\Lambda}I_\alpha(\Lambda,\alpha) + \pi\sin[\Lambda(\alpha-1)\pi]\sinh[\Lambda(\alpha-1)\pi]\frac{\sin(\Lambda\pi)^2-\sinh(\Lambda\pi)^2}{\sin(\Lambda\pi)\sinh(\Lambda\pi)}. \tag{5.18}$$

Therefore, I_α and I_Λ are everywhere different from zero on C_I and

$$I_\alpha \cdot I_\Lambda > 0 \quad \text{for every } (\alpha,\Lambda)\in C_I\,; \tag{5.19}$$

the sign in (5.19) is obtained on C_I^0 by using (5.15) and (5.17), while on $C_I\setminus C_I^0$ we see that (5.16) and (5.18) both have the sign of $-\sin(\Lambda\pi)\sin[\Lambda(\alpha-1)\pi]$. As for (5.18), notice that the second summand therein has the same sign as the first. Thus (5.19) follows and, by the Implicit Function Theorem, the curves depicted in Figure 9 are graphs of an analytic function $\Lambda=\Lambda(\alpha)$ in any neighborhood of each point of C_I; moreover, the function $\alpha\mapsto\Lambda(\alpha)$ is strictly decreasing in view of (5.19).

The statement for even eigenfunctions can be obtained by reasoning in an analogous way on the function P, changing C_I^0 with $C_P^0 := C_P\cap\Big\{(\alpha,\Lambda)\mid \Lambda-\frac{1}{2}\in\mathbb{N}\Big\}$. □

We now determine the limits of the function $\alpha\mapsto\Lambda(\alpha)$ for $\alpha\to 1$ and $\alpha\to+\infty$.

Lemma 16. *For any curve $\Lambda=\Lambda(\alpha)$ whose graph is a connected subset of C_I or C_P, there exists a unique $n\in\mathbb{N}$ such that*

$$\lim_{\alpha\to 1^+}\Lambda(\alpha)=\Lambda_n. \tag{5.20}$$

Moreover, this correspondence is one-to-one.

Proof. We restrict again our attention to odd eigenfunctions, the arguments for the even ones being similar. Since $\alpha\mapsto\Lambda(\alpha)$ is strictly decreasing by Lemma 15, the limit in (5.20) exists and we denote it by $\hat\Lambda$. To compute $\hat\Lambda$, we analyze the behavior of $\Lambda(\alpha)$ in a neighborhood of the point $(\alpha,\Lambda)=(1,\hat\Lambda)$, parametrizing its graph as the curve

$$\Lambda(s)=\hat\Lambda+l(s),\quad \alpha(s)=1+\beta(s),\quad (s\geqslant 0),\quad l(0)=\beta(0)=0.$$

We first notice that

$$\frac{\sin[\Lambda\beta(s)\pi]}{\sinh[\Lambda\beta(s)\pi]} = 1+o(1)\qquad \text{as } s\to 0.$$

Therefore, if we perform an asymptotic expansion of the identity $I(\alpha(s),\Lambda(s))\equiv 0$ as $s\to 0$, we obtain

$$\sin\big[(\hat\Lambda+l(s))(1+\beta(s))\pi\big]\sinh\big[(\hat\Lambda+l(s))\pi\big] = \sinh\big[(\hat\Lambda+l(s))(1+\beta(s))\pi\big]\sin\big[(\hat\Lambda+l(s))\pi\big](1+o(1)).$$

Introducing the infinitesimal $\varepsilon(s):=l(s)+\hat\Lambda\beta(s)$, the last identity reads

$$\Big(\sin\big[\hat\Lambda\pi\big]+\cos\big[\hat\Lambda\pi\big]\varepsilon(s)\pi+o(\varepsilon(s))\Big)\Big(\sinh\big[\hat\Lambda\pi\big]+\cosh\big[\hat\Lambda\pi\big]l(s)\pi+o(\varepsilon(s))\Big)$$

$$=\Big(\sinh\big[\hat\Lambda\pi\big]+\cosh\big[\hat\Lambda\pi\big]\varepsilon(s)\pi+o(\varepsilon(s))\Big)\Big(\sin\big[\hat\Lambda\pi\big]+\cos\big[\hat\Lambda\pi\big]l(s)\pi+o(\varepsilon(s))\Big)(1+o(1)).$$

After computing all the products, some terms cancel. Then, by dropping the lower order terms and by recalling that $I(\alpha,\Lambda)\equiv 0$, we obtain

$$\frac{\sin(\hat\Lambda\pi)}{\sinh(\hat\Lambda\pi)}=\frac{\cos(\hat\Lambda\pi)}{\cosh(\hat\Lambda\pi)},$$

namely $\hat{\Lambda}^4$ satisfies (3.7) and therefore it is an odd eigenvalue of (3.6).

We now prove that for every eigenvalue Λ_n of the clamped problem (3.6) there exists exactly one connected branch of eigenvalues of (3.2) emanating from it. We consider the hyperbolas

$$\mathcal{H}_n = \{(\alpha, \Lambda) \mid \Lambda\alpha = n\}, \quad n \in \mathbb{N}.$$

From (3.7) we deduce that for every couple of consecutive integers n and $n+1$, there exists a unique odd eigenvalue $\hat{\Lambda}$ of the clamped problem (3.6) such that $(1, \hat{\Lambda})$ belongs to the region delimited by $\mathcal{H}_n$ and $\mathcal{H}_{n+1}$: precisely, $\hat{\Lambda} = \Lambda_{2n-1}$. Moreover, since

$$I(\alpha,\Lambda) = \sin(\Lambda\alpha\pi)\big[\sinh(\Lambda\pi)\sinh[\Lambda(\alpha-1)\pi] - \sinh(\Lambda\alpha\pi)\sin(\Lambda\pi)\cos(\Lambda\pi)\big] + \sinh(\Lambda\alpha\pi)\sin^2(\Lambda\pi)\cos(\Lambda\alpha\pi)$$

changes sign passing from $\mathcal{H}_n$ to $\mathcal{H}_{n+1}$, there exists at least one curve $\Lambda = \Lambda(\alpha)$ of solutions of $I(\alpha, \Lambda) = 0$ included therein. In fact, such a curve is unique, since formula (5.18) implies that on each branch emanating from $(1, \Lambda_{2n-1})$ the function I_Λ has strictly the same sign: this would be a contradiction in presence of multiple branches, since on each branch it is $I(\alpha, \lambda) = 0$. □

Lemmas 15 and 16 prove all the statements of Theorem 8' and thus all the ones of Theorem 8, except the limit $\lambda_n(a) \to \Lambda_n^*$ for $a \to 0$. For even eigenfunctions, the limit is obtained simply by letting $a \to 0$ in (3.4), noticing that the limit equation is the one defining the eigenvalues Λ_n^* (recall (3.7) and (3.10)). For odd eigenfunctions, this does not work since it produces an identity; the thesis instead follows from the just proved fact that $\lambda_n(a) \to \Lambda_n$ for $a \to 1$ (Lemma 16), together with the invariance of (3.3) upon the substitution $a \mapsto 1 - a$.

5.5 Proof of Theorem 10

As in the proof of Theorem 8, we work with the variables $\Lambda = \lambda a$ and $\alpha = 1/a$. In view of Theorem 8, we can sort the eigenvalues of (5.12) in increasing order $\{\Lambda_0, \Lambda_1, \Lambda_2, \ldots\}$ and label the corresponding eigenfunctions again as $\{e_0, e_1, e_2, \ldots\}$. Theorem 10 is now rephrased as follows.

Theorem 10'. *For $\alpha > 1$, it holds that $i(e_n) = n$, for every $n = 0, 1, 2, \ldots$. Moreover, as α increases, the zeros of $e_n = e_{\Lambda_n(\alpha)}$ move by couples from the central span to the side spans whenever the curve $\Lambda = \Lambda_n(\alpha)$ intersects any of the horizontal lines $\{\Lambda = \Lambda_k\}$, for integers $k \geqslant 0$ having the same parity as n.*

The nice properties of the curves $\Lambda = \Lambda(\alpha)$, which we visualize in Figure 18, bring further evidence of the convenience of the change of variables made above.

To prove Theorem 10', we fix the notations

$$k_o(\Lambda) = \left[\Lambda - \frac{1}{2}\right], \qquad k_e(\Lambda) = [\Lambda], \qquad r(\Lambda) = \left[\Lambda(\alpha - 1) - \frac{1}{2}\right], \tag{5.21}$$

where $[\cdot]$ denotes the integer part and is set equal to 0 for negative numbers. Moreover, we introduce the two functions

$$g(s) = \frac{\sin(s\pi)}{\sinh(s\pi)} - \frac{\cos(s\pi)}{\cosh(s\pi)}, \qquad h(s) = \frac{\sin(s\pi)}{\sinh(s\pi)} + \frac{\cos(s\pi)}{\cosh(s\pi)}.$$

With these preliminaries, we first state a technical result.

Lemma 17. *Let $\alpha > 1$ be fixed. Let $\mu = \Lambda^4$ be an eigenvalue of (5.12), with corresponding eigenfunction e_Λ. If e_Λ is* odd*, then its number of zeros in J_0 is*

$$\begin{aligned}
&2k_o(\Lambda) + 1 \text{ if } g(\Lambda) < 0, \qquad 2k_o(\Lambda) + 3 \text{ if } g(\Lambda) > 0, \qquad \text{when } k_o(\Lambda) \text{ is odd;}\\
&2k_o(\Lambda) + 1 \text{ if } g(\Lambda) > 0, \qquad 2k_o(\Lambda) + 3 \text{ if } g(\Lambda) < 0, \qquad \text{when } k_o(\Lambda) \text{ is even.}
\end{aligned}$$

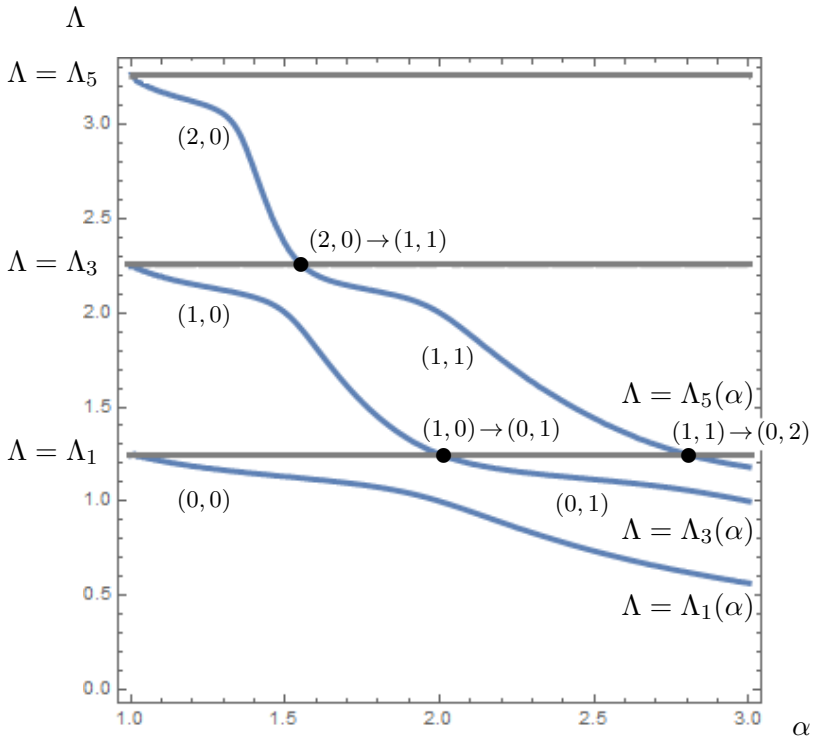

Figure 18: A visual description of Theorem 8' for odd eigenfunctions.

If e_Λ *is* even*, then its number of zeros in* J_0 *is*

$$\begin{array}{lll} 2k_e(\Lambda) \text{ if } h(\Lambda) < 0, & 2k_e(\Lambda) + 2 \text{ if } h(\Lambda) > 0, & \text{when } k_e(\Lambda) \text{ is odd;} \\ 2k_e(\Lambda) \text{ if } h(\Lambda) > 0, & 2k_e(\Lambda) + 2 \text{ if } h(\Lambda) < 0, & \text{when } k_e(\Lambda) \text{ is even.} \end{array}$$

Finally, the number of zeros of e_Λ *in* J_- *(and thus in* J_+*) is*

$$\begin{array}{lll} r(\Lambda) \text{ if } g[\Lambda(\alpha-1)] < 0, & r(\Lambda) + 1 \text{ if } g[\Lambda(\alpha-1)] > 0, & \text{when } r(\Lambda) \text{ is odd;} \\ r(\Lambda) \text{ if } g[\Lambda(\alpha-1)] > 0, & r(\Lambda) + 1 \text{ if } g[\Lambda(\alpha-1)] < 0, & \text{when } r(\Lambda) \text{ is even.} \end{array}$$

Proof. We carry on a detailed proof only for odd eigenfunctions, the argument for the even ones being similar. In this case, $x = 0$ is a zero of e_Λ in J_0; on this interval, we thus restrict our attention to the sub-interval $(0, \pi)$. Therein, the zeros of e_Λ correspond to the zeros of the function

$$\zeta(x) := \frac{\sin(\Lambda x)}{\sinh(\Lambda x)} - \frac{\sin(\Lambda \pi)}{\sinh(\Lambda \pi)},$$

which we now count by focusing on the behavior of the sine-function appearing in the numerator. To this end, observe first that $\zeta(x)$ is decreasing and positive for $x \in (0, \pi/2\Lambda]$. Therefore, if $\Lambda \leqslant 1/2$ then $\zeta(x) > 0$ for every $x \in (0, \pi)$, otherwise $\zeta(x) > 0$ for every $x \in (0, \pi/2\Lambda)$. In the former case, $k_o(\Lambda) = 0$ and the statement is proved since $\tan(\Lambda\pi) > \tanh(\Lambda\pi)$ for $\Lambda \in (0, 1/2]$. In the latter case, in any interval of the kind $[(2s+1)\pi/2\Lambda, (2s+3)\pi/2\Lambda]$, with $s \geqslant 0$ integer (corresponding to a "half-cycle" of the sine function between two consecutive extremal values), $\zeta(x)$ has exactly one zero in view of the Intermediate Value Theorem. Since there are exactly $k_o(\Lambda)$ such intervals strictly contained in $(0, \pi)$, we obtain $k_o(\Lambda)$ zeros in $(0, \pi)$. We then find at least $2k_o(\Lambda) + 1$ zeros in J_0; however, there may be another zero in the "residual" interval $R = ((2k_o(\Lambda) + 3)\pi/2\Lambda, \pi)$, where the sine function does not perform a complete half-cycle. Indeed, since $\zeta(\pi) = 0$, there is a additional zero in $(0, \pi)$ if and only if

ζ has in R a local extremum with opposite sign with respect to $\zeta((2k_o(\Lambda)+3)\pi/2\Lambda)$. This happens if and only if $e'_\Lambda(\pi^-)<0$, so that $g(\Lambda)>0$ when k_o is odd, and $e'_\Lambda(\pi^-)>0$, so that $g(\Lambda)<0$ when k_o is even. Similar arguments prove the statement for the lateral spans. This completes the proof of the lemma. □

In Lemma 17 we have not considered the cases when $g(\Lambda)=0$ or $h(\Lambda)=0$ (and similar conditions on the lateral spans). This is due to the fact that

$$e_\Lambda(\pm\pi)=e'_\Lambda(\pm\pi)=0, \text{ that is, a double zero appears in the piers} \quad\Longleftrightarrow\quad g(\Lambda)h(\Lambda)=0. \tag{5.22}$$

Indeed, it is immediate to check that (5.22) may be fulfilled only for the eigenfunctions $\mathscr{O}_\Lambda$ and $\mathscr{E}_\Lambda$ for which, respectively, such condition reads

$$g(\Lambda)=0 \quad \text{and} \quad g[\Lambda(\alpha-1)]=0,$$

$$h(\Lambda)=0 \quad \text{and} \quad g[\Lambda(\alpha-1)]=0.$$

We continue the proof of Theorem 10, carrying on the details only for odd eigenfunctions, the case of even eigenfunctions being similar. Let Λ_{2m+1} be an odd eigenvalue of (3.6) for some integer $m\geqslant 0$. The strategy is to start from the point $(1,\Lambda_{2m+1})$ of the (α,Λ)-plane and to show that the number of zeros along the branch $(\alpha,\Lambda(\alpha))$ is constant, so that it equals $\#\{x\in J_0 \mid \psi_{2m+1}(x)=0\}=2m+1$ as can be checked by recalling (3.8); here, $\alpha\mapsto\Lambda(\alpha)$ is the function found and characterized in Theorem 8'.

To this end, we introduce some notations. We define the open strips determined by the horizontal lines $\{\Lambda=\Lambda_{2k+1}\}$ in the (α,Λ)-plane, that is,

$$R_0=\mathbb{R}_+\times(0,\Lambda_1), \qquad R_k=\mathbb{R}_+\times(\Lambda_{2k-1},\Lambda_{2k+1}), \qquad k=1,2,3,\dots; \tag{5.23}$$

notice that, since $\Lambda_n\approx n/2+3/4$ by (3.7), such strips contain one horizontal line corresponding to an integer Λ; more precisely, the line $\{\Lambda=k\}$ is contained in R_{k-1}.

We denote by $\mathcal{C}_{2m+1}$ the branch $(\alpha,\Lambda(\alpha))$ that begins at $(1,\Lambda_{2m+1})$ and continues in the direction of increasing α and, for $k\leqslant m$, we set $\mathcal{C}^k_{2m+1}:=\mathcal{C}_{2m+1}\cap R_k$. Notice that, recalling (3.7), it holds

$$\operatorname{sgn} g(\Lambda)=(-1)^k \quad \text{ on } \mathcal{C}^k_{2m+1}. \tag{5.24}$$

By (5.22), we know that in correspondence of $\mathcal{C}_{2m+1}\cap\{\Lambda=\Lambda_{2k+1}\}$ the eigenfunction $e_{\Lambda(\alpha)}$ displays a double zero in the piers. By (3.7) and (3.8), we have that $\Lambda_{2m+1}\approx m+5/4$ and ψ_{2m+1} has $2m+1$ zeros in J_0. Hence, if $\alpha-1$ is sufficiently small, by continuity it turns out that $k_o(\Lambda)=k_o(\Lambda_{2m+1})$ and $r(\Lambda)=0$: therefore, the numbers of zeros on the central span J_0 and on the lateral spans $J_\pm$ are maintained equal to $2m+1$ and 0, respectively, in a neighborhood of $(1,\Lambda_{2m+1})$ while following $\mathcal{C}_{2m+1}$ (notice that g has constant sign on $\mathcal{C}^m_{2m+1}$, that $g[\Lambda(\alpha-1)]>0$ for α close to 1 and that the procedure to count the number of zeros in J_0 used to prove Lemma 17 holds as well for the eigenfunctions of the clamped problem on $[-\pi,\pi]$). By Lemma 17, on growing of α these numbers are ruled by the maps $k_o(\Lambda(\alpha))$ and $r(\Lambda(\alpha))$ defined in (5.21); indeed, in view of (3.7), following the (decreasing) branch $\mathcal{C}_{2m+1}$ the curve $\Lambda=\Lambda(\alpha)$ alternatively crosses the lines $\{\Lambda=n+1/2\}$ for integers $n\leqslant m$, and $\{\Lambda=\Lambda_{2k+1}\}$ for integers $k<m$. The following lemmas detect the changes in the number of zeros of the eigenfunctions on each span in correspondence of such crossings.

Lemma 18. *The number of zeros of $e_{\Lambda(\alpha)}$ in J_0 decreases by 2 at each crossing of $\Lambda=\Lambda(\alpha)$ with the lines $\{\Lambda=\Lambda_{2k+1}\}$, elsewhere it does not vary.*

Proof. Recalling (5.24), we see that whenever the branch $\Lambda=\Lambda(\alpha)$ crosses the lines $\Lambda=\Lambda_{2k+1}$, $k<m$, the integer $k_o(\Lambda)$ remains constant but $g(\Lambda)$ changes sign, so that the number of zeros on J_0 changes from $2k_o(\Lambda)+3$ to $2k_o(\Lambda)+1$. This proves the first part of the statement.

On the other hand, any crossing with the lines $\{\Lambda = n + 1/2\}$ does not modify the total number of zeros in the spans, since in this case $k_o(\Lambda)$ changes parity but $g(\Lambda)$ maintains the same sign. To see this, assume first that m is odd; then, the sign of $g(\Lambda)$ is negative in view of (5.24), implying that above the line $\Lambda = n + 1/2$ it is $k_o(\Lambda) = m$ (odd) and the corresponding e_Λ has $2k_o(\Lambda) + 1 = 2m + 1$ zeros, and below such line $k_o(\Lambda) = m - 1$ (even) and e_Λ possesses $2k_o(\Lambda) + 3 = 2(m - 1) + 3 = 2m + 1$ zeros. If m is even, a similar argument holds. □

Lemma 19. *The numbers of zeros of $e_{\Lambda(\alpha)}$ in J_- and in J_+ both increase by one unit at every crossing of $\Lambda = \Lambda(\alpha)$ with the lines $\{\Lambda = \Lambda_{2k+1}\}$, elsewhere they do not vary.*

Proof. We begin by stating three facts which follow from some calculus arguments. For the sake of brevity, we only give a hint of their proof.

Fact (I). *The hyperbolas*

$$\mathcal{H}_n = \left\{(\alpha, \Lambda) \in \mathbb{R}^2_+ \mid \Lambda\alpha = n\right\}, \quad n = 1, 2, \dots,$$

are such that $\mathcal{C}_{2m+1}$ is contained in the region between $\mathcal{H}_{m+1}$ and $\mathcal{H}_{m+2}$ and is tangent to $\mathcal{H}_{m+2}$, see the left picture in Figure 19. The tangency points correspond to couples (α, Λ) for which $e_\Lambda \in C^4(\overline{J})$.

To prove this, one can change variables by introducing the homeomorphism

$$\Phi : (1, +\infty) \times (0, +\infty) \to \{(x, y) \in \mathbb{R}^2_+ \mid x > y\}, \quad (x, y) = \Phi(\alpha, \Lambda) = (\Lambda\alpha\pi, \Lambda\pi), \tag{5.25}$$

so as to straighten the hyperbolas $\mathcal{H}_n$, which become vertical lines, see the right picture in Figure 19. One can then check that $\Phi(\mathcal{C}_{2m+1})$ is contained in the region between $\Phi(\mathcal{H}_{m+1})$ and $\Phi(\mathcal{H}_{m+2})$ and that it is tangent to $\Phi(\mathcal{H}_{m+2})$. The second part of the statement follows from the fact that $\Lambda\alpha = \lambda$.

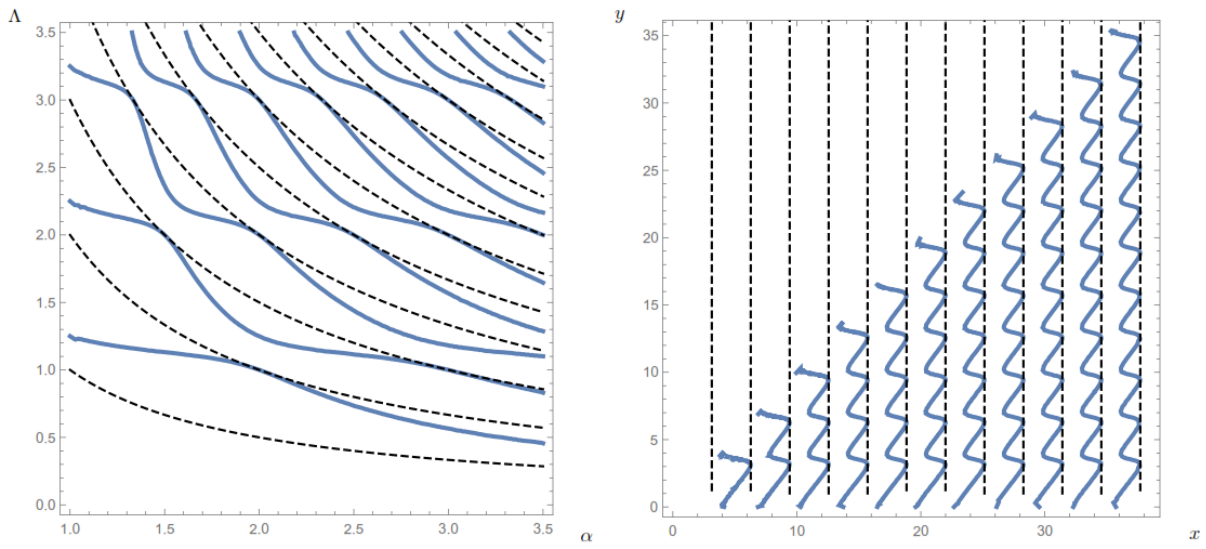

Figure 19: The hyperbolas $\mathcal{H}_n$ (left, dashed) and their images (right) through the map Φ in (5.25).

Fact (II). *On the branch $\alpha \mapsto \Lambda(\alpha)$, it holds* $\operatorname{sgn} g[\Lambda(\alpha - 1)] = -\operatorname{sgn}[g(\Lambda)\sin(\Lambda\alpha\pi)]$, *so that*

$$\operatorname{sgn} g[\Lambda(\alpha - 1)] = (-1)^{m+k+2} \quad \text{on } \mathcal{C}^k_{2m+1},$$

implying in particular

$$g[\Lambda(\alpha - 1)] > 0 \quad \text{on } \mathcal{C}^m_{2m+1}.$$

This follows by rewriting (5.13) as

$$\sin(\Lambda\pi)\sinh(\Lambda\pi)(\cos[\Lambda(\alpha-1)\pi]\sinh[\Lambda(\alpha-1)\pi]-\cosh[\Lambda(\alpha-1)\pi]\sin[\Lambda(\alpha-1)\pi])=$$
$$\sin[\Lambda(\alpha-1)\pi]\sinh[\Lambda(\alpha-1)\pi](\sin(\Lambda\pi)\cosh(\Lambda\pi)-\cos(\Lambda\pi)\sinh(\Lambda\pi)),$$

and using (5.24) and Fact (I), which says that

$$\operatorname{sgn}\sin(\Lambda\alpha\pi)=(-1)^{m+1}\quad\text{ on }\mathcal{C}_{2m+1}.$$

Fact (III). *The hyperbola*

$$\widetilde{\mathcal{H}}_n=\left\{(\alpha,\Lambda)\in\mathbb{R}^2_+\mid\Lambda(\alpha-1)=n+\frac{1}{2}\right\},\quad n=0,1,\dots$$

crosses $\mathcal{C}_{2m+1}$ if and only if $n\leqslant m$. In this case, the intersection between $\widetilde{\mathcal{H}}_n$ and $\mathcal{C}_{2m+1}$ is unique and takes place in the strip R_{m-n} (recall the notation introduced in (5.23)*).*

This is quite evident in the left picture in Figure 20. Through the change of variables Φ defined in (5.25) one may again straighten the considered hyperbolas, as displayed in the right picture in Figure 20. Then one rewrites (5.13) in this new coordinate system as

$$\sin(x)\sinh(y)\sinh(x-y)=\sinh(x)\sin(y)\sin(x-y).\tag{5.26}$$

Noticing that the regions $\Phi(R_k)$ remain horizontal strips, while the vertical lines $\Phi(\mathcal{H}_n)$ depicted in the right picture in Figure 19 determine lower and upper bounds for x on each transformed branch $\Phi(\mathcal{C}_{2m+1})$, one can then show that there exists a unique intersection between $\Phi(\widetilde{\mathcal{H}}_n)$ and $\Phi(\mathcal{C}_{2m+1})$ for x within such bounds. This may be done rigorously by combining equation (5.26) with $x-y=(n+1/2)\pi$: existence and uniqueness of the solutions of this system follow from monotonicity arguments. Notice that, in correspondence of the hyperbola $\widetilde{\mathcal{H}}_n$, the number $r(\Lambda)$ changes.

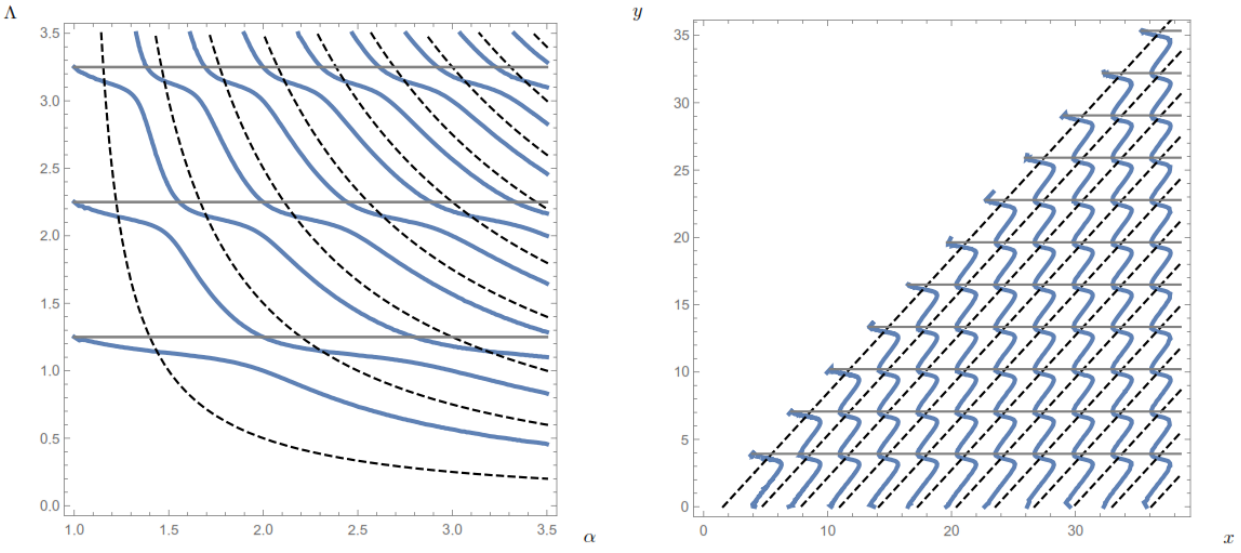

Figure 20: The hyperbolas $\widetilde{\mathcal{H}}_n$ and their straightening through the map Φ in (5.25).

With these three facts, we can now complete the proof of the statement. In the strip R_m, the branch $\mathcal{C}_{2m+1}$ crosses the hyperbola $\widetilde{\mathcal{H}}_0$ thanks to Fact (III) but, according to Lemma 17, no zeros appear in the lateral span in correspondence of such intersection, since $r(\Lambda)$ remains equal to 0 and $g[\Lambda(\alpha-1)]>0$ on

$\mathcal{C}^m_{2m+1}$. Thanks to this fact and with a similar argument, using again Lemma 17 it is possible to show that *none* of the crossings with the hyperbolas $\widetilde{\mathcal{H}}_n$ contributes to modify the number of zeros in the lateral span. Indeed, by Fact (III) the hyperbola $\widetilde{\mathcal{H}}_n$ crosses $\mathcal{C}_{2m+1}$ in R_{m-n}, with $r(\Lambda)$ passing from $n-1$ to n in correspondence of the intersection. Moreover, by Fact (II) $\operatorname{sgn} g[\Lambda(\alpha-1)] = (-1)^{2m+2-n}$ in a neighborhood of the intersection. Lemma 17 then applies, showing that the number of zeros of e_Λ in J_- and J_+ is not affected by this crossing. On the other hand, at each crossing of $\mathcal{C}_{2m+1}$ with $\{\Lambda = \Lambda_{2k-1}\}$, $k \leqslant m$, the integer $r(\Lambda)$ remains constantly equal to $m-k$, but $\operatorname{sgn} g[\Lambda(\alpha-1)]$ passes from $(-1)^{m+k+2}$ to $(-1)^{m+k+1}$, so that by Lemma 17 $e_{\Lambda(\alpha)}$ acquires a zero in J_- and a zero in J_+. □

The proof of Theorem 10' follows from Lemmas 18 and 19.

5.6 Proof of Theorem 11

From Fact (I) in the proof of Lemma 19, using the notations therein, we know that $\mathcal{C}_{2m+1}$ lies between $\mathcal{H}_{m+1}$ and $\mathcal{H}_{m+2}$, which means that

$$\lambda_{2m+1} \in [m+1, m+2]. \tag{5.27}$$

In turn, this means that any interval of the kind $[m, m+1]$ (for integer $m \geqslant 1$) contains at least an odd eigenvalue of (3.2) (namely, an eigenvalue with an odd label). By the nodal properties of the eigenfunctions stated in Theorem 10, odd and even eigenvalues alternate and so, in the interval $[m, m+2]$, there are at least three eigenvalues, two odd and one even. The thesis follows from the fact that any interval of width 3 contains an interval of the kind $[m, m+2]$ for integer m.

5.7 Proof of Theorem 13

First, reasoning as in [7, Lemma 2.2], one can see that any solution of (4.3) is of class C^∞ on each single span $\overline{I}_-$, $\overline{I}_0$ and $\overline{I}_+$, but, differently from the fourth order case (3.1), *it is not in general C^1 on the whole I*. Any solution is a linear combination of the two functions $\cos(\kappa x)$ and $\sin(\kappa x)$ on each span, so that the solutions over I are obtained by extending by symmetry

$$e(x) = \begin{cases} e_0(x) & \text{if } x \in [0, a\pi] \\ e_a(x) & \text{if } x \in [a\pi, \pi], \end{cases}$$

where $e_0 = H_0 \sin(\kappa x)$, $e_a(x) = K\cos(\kappa x) + H\sin(\kappa x)$ for odd eigenfunctions, while for the even ones it is $e_0 = K_0\cos(\kappa x)$ and $e_a(x) = K\cos(\kappa x) + H\sin(\kappa x)$. Imposing the three vanishing conditions in $a\pi$ and π, we obtain a 3×3 linear system in the unknowns H_0, K, H (or K_0, K, H) and nontrivial solutions are obtained imposing that the determinant of such system is equal to 0. All the statements of Theorem 13 are then obtained by mimicking the arguments developed in the proof of Theorem 6, with obvious changes. □

We notice that, after a change of variables $(a, \kappa) \mapsto (\alpha, K)$ similar to the one performed to prove Theorems 8 and 10, the eigenvalue problem (4.3) is transformed into

$$\int_J e'w' = \mu \int_J ew \qquad \forall w \in W(J),$$

where $J = (-\alpha\pi, \alpha\pi)$ and $W(J) := \{u \in H^1_0(J);\, u(\pm\pi) = 0\}$. In Figure 21, we depict the eigenvalues curves for such a problem; again, the change of variables seems to simplify the interpretation of the pictures.

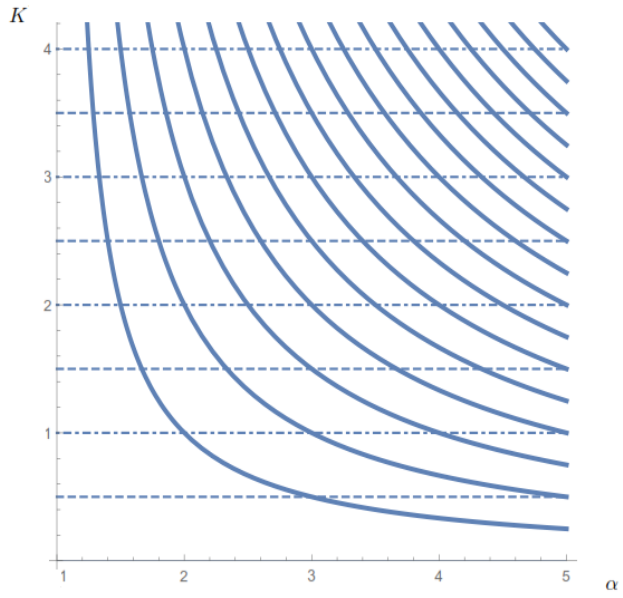

Figure 21: A pictorial description of the eigenvalues curves for (4.3), in the (α, K)-plane.

6 Conclusions

In the present paper we have introduced all the basic tools for the analysis of hinged beams with two piers. The functional and variational setting, as well as the spectral analysis, highlighted some curious phenomena such as the explicit form of the underlying functional space and the lack of regularity of weak solutions of the related equations. We showed that *each pier reduces by one the dimension of the functional space and inserts a Dirac delta within the equation.* Of particular relevance for future developments is the behavior of the eigenvalues of (3.2) as the position of the piers varies. For this reason, we gave a full picture of the behavior of the nodes of the eigenfunctions of (3.2), a feature that is essential also for engineers in order to study the oscillations of a bridge, see once again Drawing 4 in [1]. Moreover, we showed that the functional space (of codimension two) does not allow to view the fourth order eigenvalue problem (3.2) as the "squared" second order eigenvalue problem (4.3), a fact that highlights how *the stretching energy propagates in a disordered way across the piers.*

As already mentioned, this theoretical framework will be used in a forthcoming work [4], where the focus will be on the nonlinear analysis (both for beams and for degenerate plates) and on stability issues related to suspension bridges.

We finally mention two open problems related to the contents of this paper.

$\diamondsuit$ We have mainly considered the case of symmetric side spans ($b = a$). The main advantage of this restriction is that one can deal with even and odd eigenfunctions, see the discussion in Section 3. But some suspension bridges, such as the three Kurushima Bridges (see [9, Figure 2.4.6]) have asymmetric side spans. In this respect, let us also recall a forgotten suggestion from the 19th century: while commenting the collapse of the Brighton Chain Pier (1836), Russell [12] claims that *the remedies I have proposed, are those by which such destructive vibrations would have been rendered impossible.* His remedies were to alter the place of the cross bars and to put stays below the bridge which should be put *at distances not perfectly equal.* His scope was to break symmetry in the longitudinal oscillating modes of the deck. Therefore, the optimal position of the piers should also be discussed in the asymmetric framework, it is not even clear if symmetry yields better stability performances: a full analysis for the case $b \neq a$ and the comparison with symmetric side spans appears quite important and challenging.

$\diamondsuit$ Some of the results in the present paper may be extended to the case of multiple intermediate piers. This could be useful since several suspension bridges, such as the San Francisco-Oakland Bay Bridge (see [11, Fig. 15.10]), have more than two intermediate piers. With the same proof as for Theorem 1, one can show that the subspace of $H^2 \cap H_0^1(I)$ with n interior vanishing constraints has codimension n. Also Theorem 3 continues to hold with some obvious changes. However, a different and general procedure seems necessary to prove the smoothness of a solution, since problem (2.9) has exactly the same number of constraints (four) as the order of the ODE. Furthermore, the spectral analysis carried out in Section 3, including the discussion about the possible existence of positive eigenfunctions (see Figure 13) appears much longer and possibly more difficult than in the case of only two piers. In this respect, anyway, taking into account the definition of $i(e_\lambda)$ in Section 2, in presence of n piers it would be reasonable that the only positive eigenfunction is the $(n+1)$-th.

Acknowledgement. The Authors are grateful to Alberto Farina for an important remark about Theorem 3. Both the authors are supported by the Gruppo Nazionale per l'Analisi Matematica, la Probabilità e le loro Applicazioni (GNAMPA) of the Istituto Nazionale di Alta Matematica (INdAM). The second Author is also partially supported by the PRIN project *Equazioni alle derivate parziali di tipo ellittico e parabolico: aspetti geometrici, disuguaglianze collegate, e applicazioni.*

References

[1] O.H. Ammann, T. von Kármán, G.B. Woodruff, *The failure of the Tacoma Narrows Bridge*, Federal Works Agency (1941)

[2] U. Battisti, E. Berchio, A. Ferrero, F. Gazzola, *Periodic solutions and energy transfer between modes in a nonlinear beam equation*, J. Math. Pures Appl. 108, 885-917 (2017)

[3] C. Gasparetto, F. Gazzola, *Resonance tongues for the Hill equation with Duffing coefficients and instabilities in a nonlinear beam equation*, Comm. Contemp. Math. 20, 2018, 1750022 (22 pp.)

[4] M. Garrione, F. Gazzola, Nonlinear equations for beams and degenerate plates with piers, SpringerBriefs in Mathematics, Springer, Cham, 2019.

[5] F. Gazzola, R. Pavani, *Wide oscillations finite time blow up for solutions to nonlinear fourth order differential equations*, Arch. Rat. Mech. Anal. 207, 2013, 717-752

[6] B. Hartman Mather, https://a.msn.com/r/2/BBOvA55?m=nl-nl&referrerID=InAppShare&ocid=Nieuws (via Viral Hog, video)

[7] G. Holubová, A. Matas, *Initial-boundary value problem for nonlinear string-beam system*, J. Math. Anal. Appl. 288, 784-802 (2003)

[8] G. Holubová, P. Nečesal, *The Fučik spectra for multi-point boundary-value problems*, Electronic J. Diff. Eq. Conf. 18, 33-44 (2010)

[9] J.A. Jurado, S. Hernández, F. Nieto, A. Mosquera, *Bridge aeroelasticity, sensitivity analysis and optimal design*, WIT Press, Southampton (2011)

[10] J. Locker, *Self-adjointness for multi-point differential operators*, Pacific J. Math. 45, 561-570 (1973)

[11] W. Podolny, *Cable-suspended bridges*, In: Structural Steel Designers Handbook: AISC, AASHTO, AISI, ASTM, AREMA, and ASCE-07 Design Standards. By R.L. Brockenbrough and F.S. Merritt, 5^{th} Edition, McGraw-Hill, New York (2011)

[12] J.S. Russell, *On the vibration of suspension bridges and other structures; and the means of preventing injury from this cause*, Transactions of the Royal Scottish Society of Arts, Vol.1 (1841)

[13] C.E. Wilder, *Problems in the theory of ordinary linear differential equations with auxiliary conditions at more than two points*, Trans. Amer. Math. Soc. 19, 157-166 (1918)